The Canadian Mineralogist
Vol. 33, pp. 1285-1310 (1995)

THE OCCURRENCE OF GOLD IN SULFIDE DEPOSITS OF THE TAG HYDROTHERMAL FIELD, MID-ATLANTIC RIDGE*

MARK D. HANNINGTON
Geological Survey of Canada, 601 Booth Street, Ottawa, Ontario K1A 0E8

MARGARET K. TIVEY
Woods Hole Oceanographic Institution, Woods Hole, Massachusetts 02543, U.S.A.

ADRIENNE C.L. LAROCQUE
Department of Geological Sciences, University of Manitoba, Winnipeg, Manitoba R3T 2N2

SVEN PETERSEN
Institute for Mineralogy, Technical University, Bergakademie, D-09596 Freiberg, Germany

PETER A. RONA
Institute of Marine Sciences, Rutgers University, Rutgers, New Jersey 08903-0231, U.S.A.

Abstract

Sulfide deposits in the TAG Hydrothermal Field include both active and relict hydrothermal mounds, with high-temperature black smokers, lower-temperature white smoker chimneys, and coarse recrystallized massive sulfides. On the active TAG mound, black smoker chimneys consist mainly of pyrite–chalcopyrite assemblages (up to 24 wt.% Cu), with concentrations of gold from 0.03 to 1.7 ppm Au. Zn-rich sulfides from the mound are commonly gold-rich, with an average of 9.5 ppm Au and a median value of 6.0 ppm Au ($n = 15$). White smokers from a low-temperature vent complex on the mound have gold contents of up to 42 ppm Au. In the white smokers, gold is present as submicroscopic particles or as "invisible" gold within fine-grained dendritic sphalerite that comprises the bulk of the chimneys. The significant enrichment of gold within the lower-temperature white smoker complex and the effective separation of Zn and Cu in hydrothermal precipitates at the surface of the mound are interpreted to reflect a strong thermal gradient within the central zone of upflow. Massive, Cu–Fe–Zn sulfides from a nearby relict sulfide mound, the MIR Mound, also are gold-rich. Concentrations of gold in the MIR sulfides reach 15.5 ppm Au, with an average of 7.6 ppm and a median value of 7.7 ppm ($n = 13$). These samples are distinctly coarse-grained and show evidence of extensive hydrothermal recrystallization and replacement, as well as of overprinting by multiple hydrothermal events. Native gold in these samples occurs mainly as free grains up to 4 μm in diameter, occupying open spaces in the massive sulfides, in late microfractures, and along grain boundaries between coarse recrystallized sulfides. Ion-microprobe analyses of pyrite and chalcopyrite indicate background concentrations of less than 2 ppm Au as invisible gold in the coarse-grained sulfides. The most abundant gold occurs in a late-stage, sphalerite-rich vein that cuts earlier massive pyrite; similar veins may have been feeders for gold-rich white smokers once present at the surface of the mound (*i.e.*, similar to those on the active TAG Mound). A history of high-temperature venting in the TAG Hydrothermal Field, spanning more than 50,000 years, has resulted in extensive hydrothermal reworking of the sulfide deposits. This process is considered to be important for the remobilization and local reconcentration of early-formed gold and may have been responsible for the formation of relatively coarse-grained, high-purity native gold in recrystallized massive sulfides from the MIR Mound.

Keywords: native gold, seafloor sulfides, Mid-Atlantic Ridge, TAG Hydrothermal Field, black smokers, white smokers, hydrothermal reworking.

Sommaire

Les gisements de sulfures du champ d'activité hydrothermale de TAG, sur la crête médio-atlantique, comprennent à la fois des amoncellements hydrothermaux actifs et éteints, des fumeurs noirs actifs à température élevée, des fumeurs blancs actifs à plus faible température, et des amas de sulfures massifs recristallisés, à grains grossiers. A cet endroit, les cheminées associées aux fumeurs noirs sont faites d'assemblages à pyrite + chalcopyrite (avec jusqu'à 24% de Cu en poids) ayant des teneurs en or

* Geological Survey of Canada contribution number 68294.

allant de 0.03 à 1.7 ppm. Les sulfures riches en Zn sont généralement riches en or, avec en moyenne 9.5 ppm et une valeur médiane de 6.0 ppm (n = 15). Les fumeurs blancs, qui font partie du complexe d'évents à faible température, contiennent jusqu'à 42 ppm Au. L'or y est présent sous forme de particules sub-microscopiques ou d'or "invisible" dans la sphalérite dendritique à granulométrie fine qui constitue la majeure partie des cheminées. L'enrichissement important en or dans les évents de faible température et la séparation importante du Zn et du Cu dans les précipités hydrothermaux à la surface de l'amoncellement seraient favorisés par la présence d'un fort gradient thermique au sein de la zone centrale de flux vertical. Les sulfures massifs à Cu–Fe–Zn de l'amoncellement de sulfures MIR, avoisinant et maintenant éteint, sont aussi enrichis en or. Les concentrations atteignent 15.5 ppm, avec une moyenne de 7.6 ppm et une valeur médiane de 7.7 ppm (n = 13). Ces échantillons sont définitivement à granulométrie plus grossière, et témoignent d'une recristallisation hydrothermale et d'un remplacement importants, ainsi que d'une superposition d'événements hydrothermaux. Dans ces échantillons, l'or natif se présente surtout sous forme de particules libres allant jusqu'à 4 μm de diamètre; celles-ci occupent des cavités dans les sulfures massifs et des microfissures tardives, et longent les grains grossiers recristallisés. Les analyses de pyrite et chalcopyrite à la microsonde ionique indiquent des concentrations au seuil de détection, moins de 2 ppm, dans les sulfures recristallisés. Les concentrations d'or les plus élevées caractérisent une veinule tardive à sphalérite qui recoupe un amas de pyrite massif précoce. Des veines semblables pourraient représenter les filons nourriciers pour les évents de type fumeurs blancs qui ont dû être présents à la surface de l'amoncellement, par analogie à ceux en activité maintenant sur l'amoncellement TAG. Une activité hydrothermale à température élevée à TAG, étalée sur plus de 50,000 ans, a donné lieu à une recristallisation intense des gisements de sulfures. Ce processus serait d'une importance capitale pour la remobilisation et la concentration locale de l'or déposé tôt dans le système, et serait responsable de la formation de particules d'or très pur et à granulométrie relativement grossière dans les amas de sulfures recristallisés de l'amoncellement MIR.

(Traduit par la Rédaction)

Mots-clés: or natif, sulfures des fonds marins, crête médio-atlantique, champ d'activité hydrothermale TAG, fumeurs noirs, fumeurs blancs, recristallisation hydrothermale.

Introduction

The nature of primary gold mineralization in ancient massive sulfide deposits is in some cases difficult to establish owing to the effects of metamorphism, deformation and overprinting by transgressive features, which commonly contain structurally remobilized gold (*e.g.*, Larocque *et al.* 1995). Studies of the occurrence and distribution of gold in modern seafloor deposits, in particular, have helped to identify some of the primary controls on the enrichment of gold in volcanogenic massive sulfides (Hannington *et al.* 1986, Hannington & Scott 1989a, Herzig *et al.* 1993). Among the important observations made in these studies was the recognition of the low-temperature solubility of gold as aqueous sulfur complexes in active seafloor hydrothermal systems and its strong tendency to be concentrated in low-temperature vent complexes. Similar chemical models for the transport and deposition of gold were proposed for ancient deposits by Large *et al.* (1989) and Huston & Large (1989).

Mid-ocean ridge sulfide deposits have average gold contents of about 1 ppm Au, similar to those of ancient volcanogenic massive sulfides. Zn-rich assemblages are locally strongly enriched in gold, and this relationship has been documented in several deposits on the mid-ocean ridges (*e.g.*, up to 18.4 ppm Au in sphalerite from the Snakepit vent site: Hannington *et al.* 1991, Fouquet *et al.* 1993; 7 ppm Au in Zn-rich chimneys from Axial Seamount: Hannington & Scott 1988). Sulfide deposits in several of the back-arc basins of the western Pacific are also commonly gold-rich (*e.g.*, up to 28.7 ppm in a sphalerite chimney from the Lau Basin: Herzig *et al.* 1993) and exhibit similar geochemical controls on gold enrichment. In most cases, gold is strongly associated with Ag, As, Sb, and Pb, reflecting the similar behavior of these elements in solution and similar mechanisms for their precipitation (Hannington *et al.* 1991). Occurrences of significant gold in Cu-rich samples are less well documented (*e.g.*, up to 10 ppm Au in one Cu-rich sample from Escanaba Trough: Zierenberg *et al.* 1993).

Microscopic gold has been observed only rarely, for example, in the sphalerite-rich chimneys from the Lau back-arc basin (Herzig *et al.* 1993) and in metalliferous gossans where oxidation of the sulfides has caused secondary enrichment of gold (Hannington *et al.* 1988, Herzig *et al.* 1991, Fouquet *et al.* 1993). The first documented occurrence of primary native gold in sulfides from a mid-ocean ridge setting was described by Hannington *et al.* (1992) in samples collected from the TAG Hydrothermal Field, on the Mid-Atlantic Ridge (Fig. 1). Similar occurrences of native gold have since been noted in the Snakepit Hydrothermal Field, 300 km to the south (Fouquet *et al.* 1993).

In this study, the occurrence and distribution of gold have been examined in a suite of samples collected from two large active and relict sulfide deposits in the TAG Hydrothermal Field. The samples were recovered by dredging from surface and during 25 dives in 1986 and 1990. Collectively, the samples exhibit a complex paragenesis of sulfides, with multiple high-temperature hydrothermal events recorded by overprinting sulfide assemblages and complex cross-cutting relationships (*e.g.*, Rona *et al.* 1993a, Tivey *et al.* 1995). Such features are rarely documented in seafloor deposits

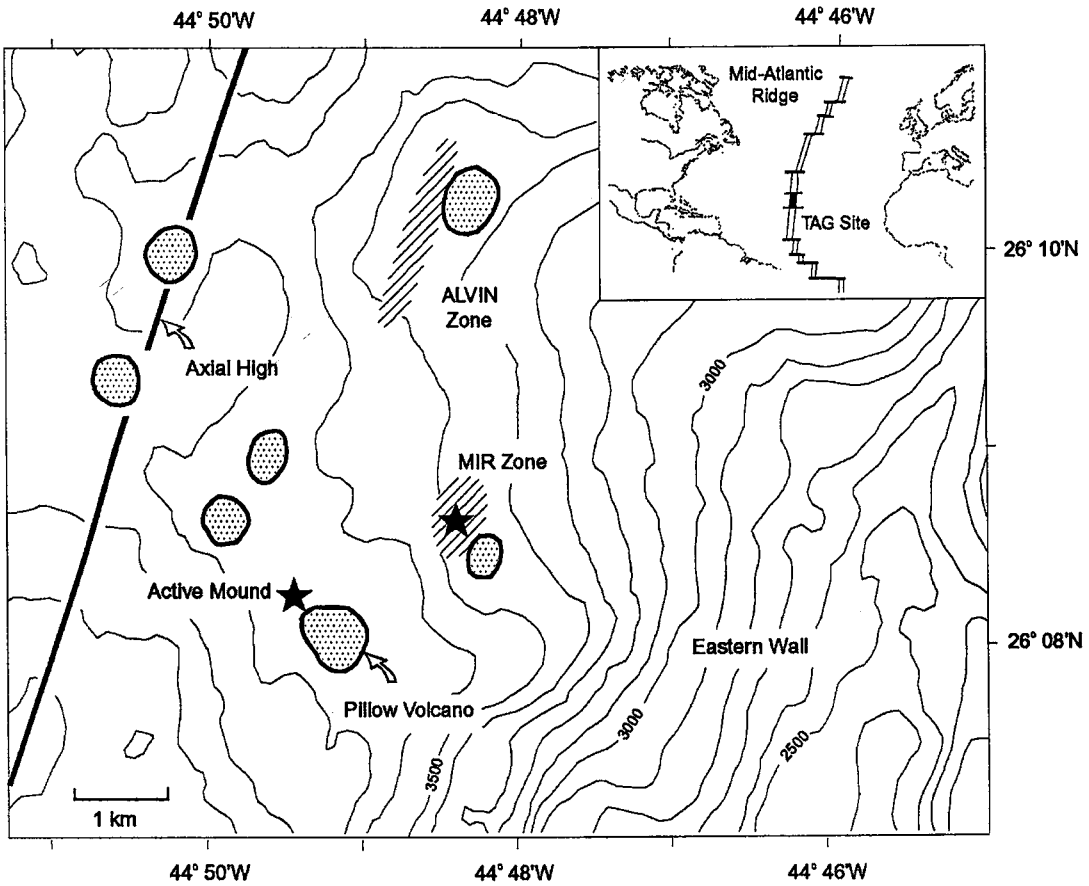

FIG. 1. Location of sulfide deposits in the TAG Hydrothermal Field (modified after Rona *et al.* 1993a, b).

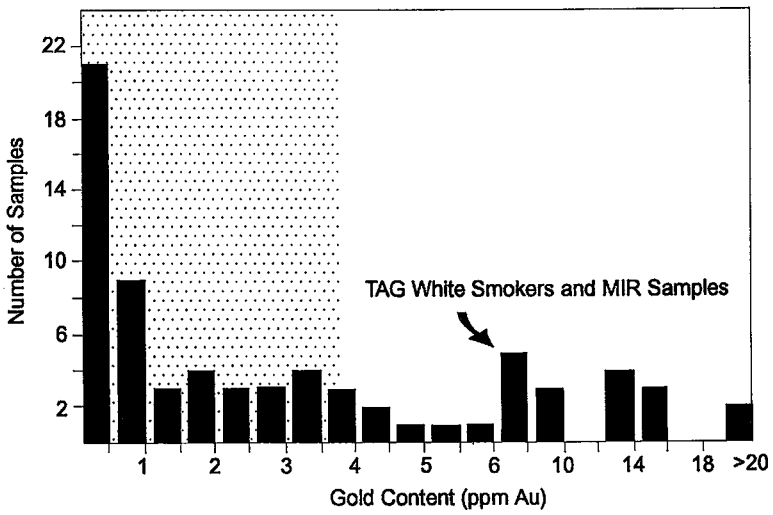

FIG. 2. Distribution of bulk gold contents in sulfide samples from the TAG Hydrothermal Field. Gold is strongly enriched in white smokers on the active TAG Mound and in hydrothermally reworked sulfides from the relict MIR Mound (shaded part indicates all other samples). Data include 27 analyses from Hannington *et al.* (1991) and 45 analyses from this study.

because sampling is often restricted to individual sulfide chimneys formed by single-stage growth or representing only the most recent phases of venting. Systematic sampling of both high- and low-temperature sulfides across the active and relict sulfide mounds in the TAG Field, and along major fault scarps and erosional surfaces that have exposed the interiors of the deposits, has made possible the partial reconstruction of the different stages of mineralization within these large deposits. Comprehensive sampling at this scale also permits a detailed assessment of the paragenesis of gold mineralization. Very high concentrations of gold have now been measured in a large number of samples from the TAG site (Fig. 2), and this study documents the nature of the gold mineralization and presents evidence for the behavior of gold during long-term hydrothermal reworking of the sulfide deposits.

Geological Setting and Description of Deposits

The TAG Hydrothermal Field is the site of several large active and fossil sulfide deposits in the rift valley and along the east wall of the Mid-Atlantic Ridge at 26°N. The sulfide deposits occur at water depths ranging from 2300 m on the wall of the valley to 4000 m at the valley floor, within an area of at least 5 km × 5 km (Rona *et al.* 1993a). The three main deposits include the actively venting TAG Mound and two former high-temperature vent fields known as the MIR Zone and the Alvin Zone (Fig. 1). The active mound is a steep-sided structure, up to 40 m in height and measuring about 250 m in diameter (Fig. 3). Hydrothermal venting is centered on a black smoker complex, 40–50 m in diameter, built on a conical

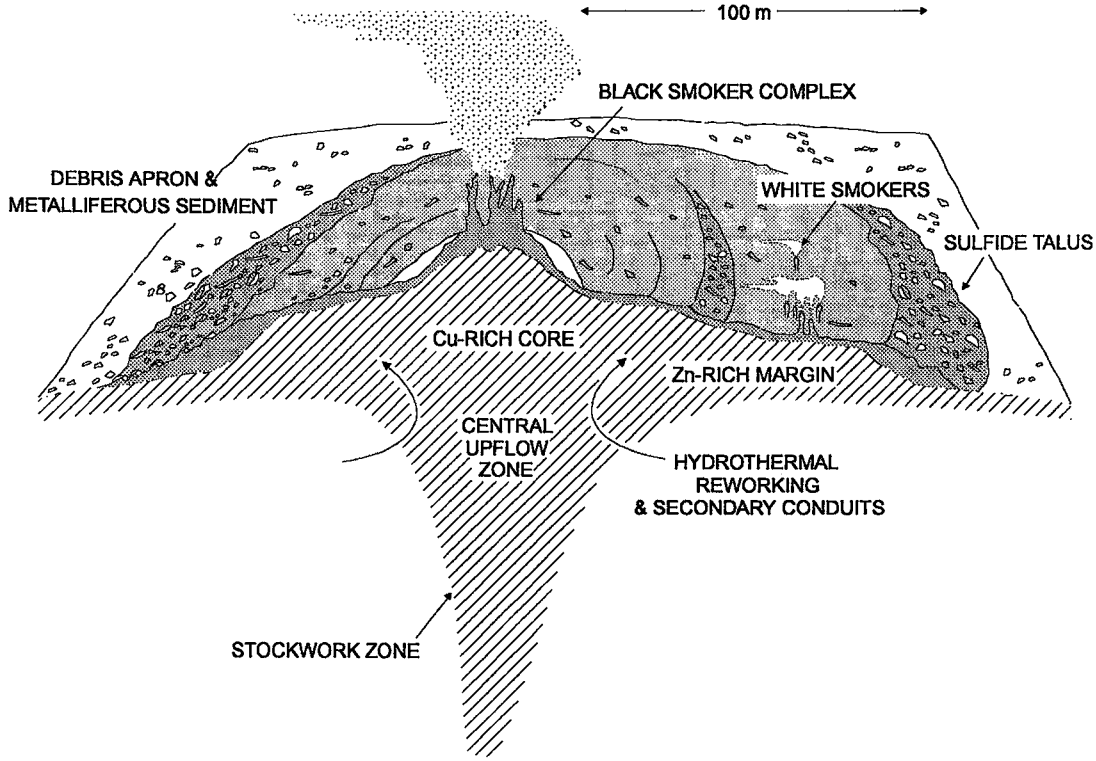

FIG. 3. Schematic section of the TAG Mound showing the distribution of active vent complexes (looking north). Most of the hydrothermal upflow is accommodated by the central black smoker complex, which is capped by multiple spire-shaped chimneys up to 15 m in height. Lower-temperature fluids are currently venting in the white smoker field and are interpreted to have been transported away from the central upflow zone through secondary conduits leading its outer margin. Individual chimneys in the white smoker field are up to 2 m in height. Cooling of hydrothermal fluids at the margins of the upflow zone results in the separation of Cu and Zn in hydrothermal precipitates at the surface and possibly within the mound. Continuous hydrothermal reworking of older sulfides may lead to a gold-enriched zone at the top of the deposit.

edifice constructed of blocks of massive pyrite, chalcopyrite and anhydrite. The black smokers are currently venting high-temperature fluids (up to 366°C) from multiple spire-shaped chimneys up to 15 m tall. The site of high-temperature discharge at the center of the mound is surrounded by a platform up to 100 m wide that is covered by sulfide debris from the frequent collapse of sulfide chimneys. The substrate is poorly exposed beneath this sulfide talus, but samples of subcropping massive sulfide crusts suggest that the bulk of the mound is composed of coarse-grained, partially recrystallized massive pyrite. Diffuse, low-temperature venting through the talus occurs over much of the surface of the mound in patchy areas up to tens of meters in diameter. A field of Zn-rich white smokers occurs near the southeastern margin of the mound (Fig. 3). The white smoker chimneys grew on top of pre-existing sulfide debris during a recent phase of hydrothermal activity and are presently discharging fluid at temperatures of 265–300°C (Thompson *et al.* 1988, Tivey *et al.* 1990). The distribution of vents across the mound indicates a well-developed thermal profile with a central zone of high-temperature upflow and a broader zone of cooler hydrothermal upflow at the margins of the deposit. The lower-temperature vent fluids in the white smoker complex are strongly depleted in sulfur compared to the black smoker fluids, suggesting that conductive cooling and precipitation of sulfides have occurred within the mound prior to venting (Edmond *et al.* 1990, Tivey *et al.* 1995). The high concentrations of Zn in these fluids have been explained by the dissolution of sphalerite and remobilization of Zn from within the mound (Edmond *et al.* 1990, Tivey *et al.* 1995). U/Th ages of sulfide samples from the active mound indicate that the current episode of high-temperature venting commenced about 50 years ago (Lalou *et al.* 1993). However, the oldest sulfides recovered from the deposit have ages between 40,000 and 56,000 years, and there is evidence for intermittent periods of high-temperature activity about every 5,000–6,000 years for the past 25,000 years (Lalou *et al.* 1990, 1993). These observations imply that early-formed sulfides within the TAG Mound may have been exposed to extensive hydrothermal reworking during the growth of the deposit.

Samples recovered from the active mound include (1) black smoker chimneys and massive pyrite–chalcopyrite assemblages from the central black smoker complex, and (2) lower-temperature white smoker chimneys and massive pyrite–sphalerite assemblages from sulfide talus on top of the mound. The black smokers consist mainly of pyrite, chalcopyrite, and anhydrite. Pyrrhotite is absent, but a primary assemblage of bornite, pyrite, and chalcopyrite has been observed in some samples. The white smokers are delicate structures with bulk porosities of up to 50 vol.%. They consist dominantly of fine-grained, dendritic and colloform sphalerite, together with minor marcasite and late-stage amorphous silica (Fig. 4). A detailed account of the mineralogy of sulfide samples from the surface of the active mound is given by Tivey *et al.* (1995). Samples of massive sulfide talus from the top of the mound commonly contain well-preserved primary banding, colloform textures, and dendritic sulfides, suggesting that much of this material was derived from the recent collapse of sulfide chimneys. However, some samples of massive sulfide talus are distinctly coarse-grained and appear to have been recrystallized. Coarse-grained, massive pyrite is also exposed by mass-wasting at the edges of the mound. This material resembles the massive sulfides from the interiors of typical Cyprus-type deposits found in ancient ophiolites (*e.g.*, Lydon 1984, Constantinou & Govett 1972, 1973, Tivey *et al.* 1992).

The MIR zone is an area of discontinuous outcrop of sulfide perched on fault blocks along the eastern wall of the rift valley, about 2 km northeast of the active TAG mound (Fig. 1). The hydrothermal deposits occupy an estimated area of about 1000 m × 900 m, but the sulfides are covered by extensive metalliferous sediment and Fe–Mn-oxide crusts. Several inactive vent-fields, containing dozens of large standing (up to 25 m in height) and toppled chimney complexes, occur along the north–south axis of the MIR zone. At the center of this zone is a large area of semicontinuous outcrop of massive sulfide exposed over a strike length of up to 600 m. The massive sulfides consist of a number of coalesced, relict mounds at different stages of weathering and mass wasting (Rona *et al.* 1990, 1993a, b). Numerous small chimneys at the center and at the margins of the main mound may be products of a recent stage of chimney growth superimposed on the older sulfides (Rona *et al.* 1993b). The last high-temperature event on the MIR Mound is estimated to have occurred about 10,000 years ago, although the initial phase of high-temperature activity in the MIR zone occurred about 100,000 years ago (Lalou *et al.* 1990, 1993). A number of high-temperature hydrothermal events at the MIR Mound, beginning about 50,000 years ago, coincided with the initiation of high-temperature venting at the presently active TAG Mound on the rift valley floor (Lalou *et al.* 1990, 1993).

Sulfide samples from the MIR zone were collected from massive sulfide outcrops exposed along talus slopes at the edge of the main mound and from large collapsed spires in nearby chimney fields. Unlike samples recovered from the TAG Mound, the sulfides from the relict MIR zone consist mainly of massive, coarse-grained Cu–Fe–Zn assemblages (Fig. 5a). The massive chalcopyrite samples are similar in bulk mineralogy to samples from the black smoker complex on the active mound and, by analogy, likely formed at high temperatures. The pyrite–marcasite and pyrite–sphalerite assemblages are similar to white smoker chimneys on the active mound and probably formed

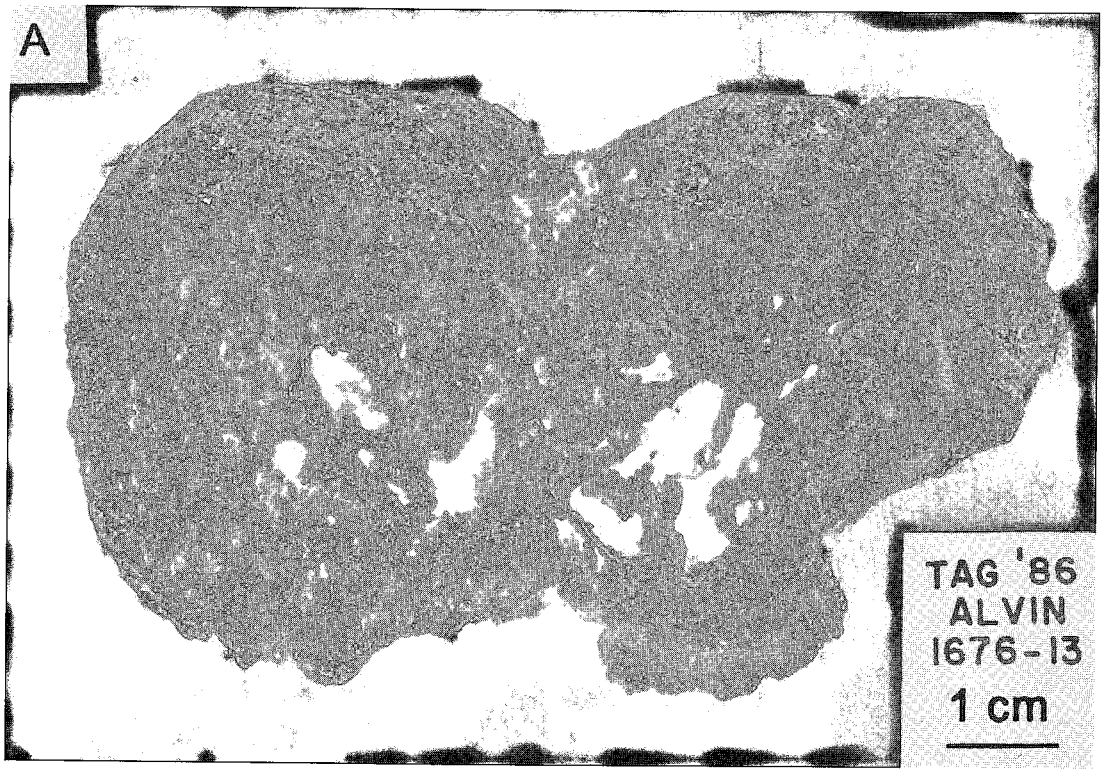
A
TAG '86
ALVIN
1676-13
1 cm

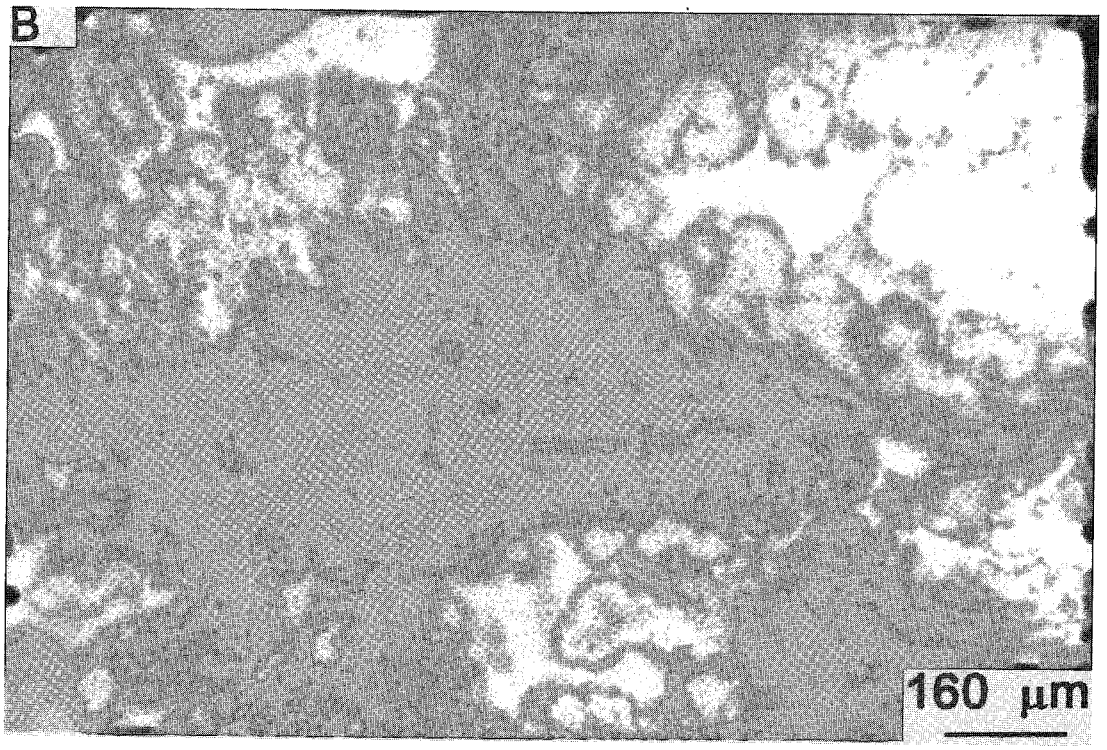
B
160 µm

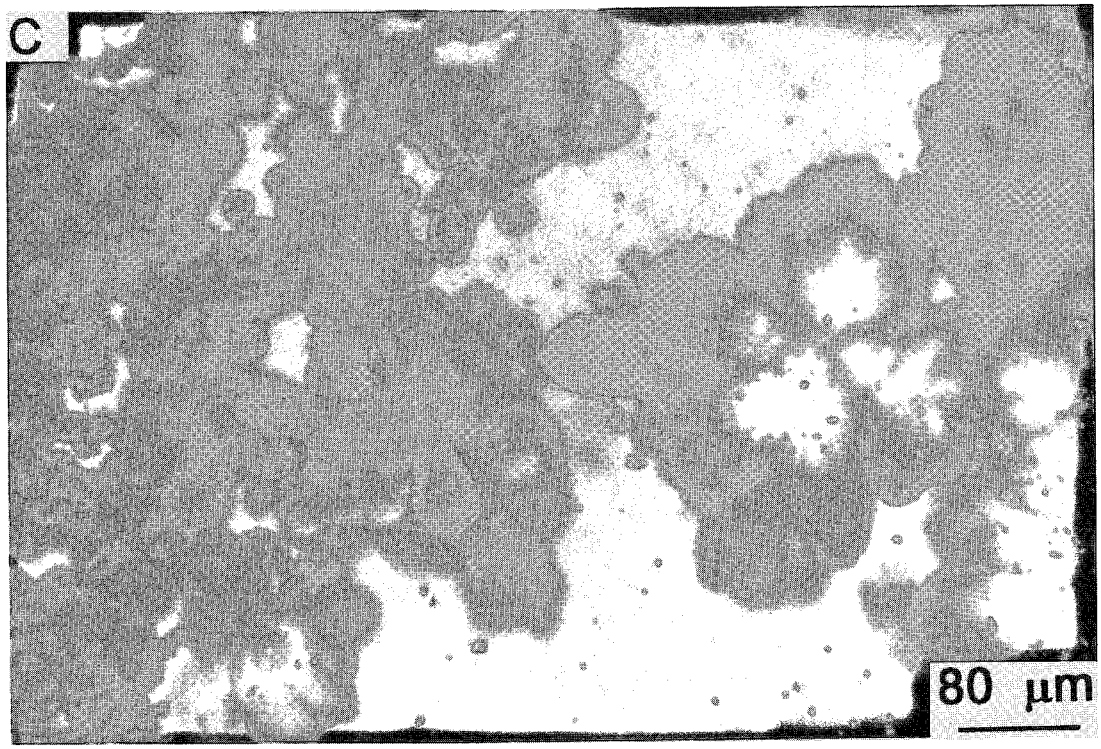

FIG. 4. Mineralogy and textures of gold-rich white smoker chimneys from the active TAG Mound. (a) Cross-section through a white smoker chimney. (b) Photomicrograph of fine-grained, dendritic sphalerite comprising the porous interior of the white smoker. Note that the sphalerite in this sample is nearly pure (<0.1 mol.% FeS) and virtually white. (c) Close-up of porous, fine-grained and dendritic sphalerite.

at much lower temperatures. Delicate, fine-grained textures typical of original chimney morphologies are preserved only locally within the largest samples or in sulfide fragments from the most recent stages of chimney growth. In large blocks of sulfide talus, however, most of the primary textures and the original porosity of the chimney material have been destroyed. Grain sizes of 1–2 mm or larger in the massive sulfides are common and suggest extensive recrystallization of the original dendritic and colloform minerals. Pyrite commonly occurs as large, poikilitic grains up to several millimeters across (Fig. 5b), locally with overgrowths of euhedral pyrite or partially replaced by later chalcopyrite. The coarse-grained nature of the sulfide minerals is in sharp contrast to the fine-grained sulfides typical of most active chimneys (*e.g.*, Bluth & Ohmoto 1988, Paradis *et al.* 1988, Hannington & Scott 1988). The continuous flow of fluids through the MIR mound during protracted, multistage hydrothermal events has led to the progressive annealing, cementation, and veining of earlier chimney debris and mound material. Non-sulfide phases, such as amorphous silica and anhydrite, which are abundant in chimneys from the active TAG Mound, are virtually absent in the MIR sulfides. These phases were likely removed during hydrothermal recrystallization, and coarse-grained massive sulfides now constitute nearly 100% of the hydrothermal assemblage, although some coarse-grained pyrite is locally cemented by late crystalline quartz. Most notably, veins of pyrite, marcasite, and sphalerite are found cross-cutting the coarse-grained, recrystallized sulfides in some samples (*e.g.*, Figs. 5b and d). Similar textures have been described in massive sulfides from other large, hydrothermally reworked sulfide deposits that have been exposed by faulting (*e.g.*, Galapagos: Embley *et al.* 1988).

Both the active TAG Mound and relict MIR Mound have well-developed surficial gossans produced by seafloor oxidation of the sulfides, and such gossans may have formed periodically throughout the long history of the deposits. This material contains abundant secondary gold concentrated by supergene processes akin to those of land-based gossans (Hannington *et al.* 1988, Herzig *et al.* 1991).

A
1 cm
B
vein
massive
pyrite-chalcopyrite
Sp
Sp
0
1
2
cm
C
pyrite
160 μm
D
sphalerite
vein
chalcopyrite
pyrite
160 μm

Sampling and Analytical Techniques

Integrated petrographic and chemical studies have been conducted on 48 bulk samples, ranging in size from 1 to 20 kg, from both the active mound and nearby relict deposits. Descriptions of 20 samples from the most recent dive series are summarized in Tables 1 and 2. From the suite of bulk samples, 72 subsamples of 1–5 grams each were selected to represent different mineralogical zones within individual chimneys and larger blocks of massive sulfide. Results for 27 subsamples from early dredging and the 1986 dive series on the active TAG Mound were presented by Hannington *et al.* (1991). Results of chemical analyses of an additional 32 subsamples from the 1990 dive series on the TAG Mound are presented in Table 3, and results for 13 subsamples from the MIR Mound are given in Table 4. Table 3 also includes results for nine duplicate subsamples chosen to evaluate the homogeneity of the most gold-rich materials. Concentrations of Fe, Zn, Au, Ag, As, Sb, Co, Se, Mo, and Cd in each sample were determined by instrumental neutron activation (NAA) at the SLOWPOKE–2 facility of the Royal Military College of Canada, Kingston, Ontario.

TABLE 1. DESCRIPTION OF SELECTED SULFIDE SAMPLES RECOVERED FROM THE ACTIVE TAG MOUND

Sample No.	Sample Type	Description	Mineralogy (modal abundances)				
			py	ccp	sp	other	
ALV2179-1	Massive sulfide crust (10 cm thick) from base of black smoker complex	Massive layers of colloform pyrite with small fluid conduits lined by chalcopyrite; with minor sphalerite	65	30	<2	tr	bornite
ALV-2179-2	Fragment of 10 m high black smoker chimney complex (363±3°C) near center of mound	Chimney with outer wall of anhydrite intergrown with minor pyrite; inner wall lined by chalcopyrite	30	30	<1	40	anhydrite
ALV2179-4	Fragment of 10 m high black smoker chimney complex (363±3°C) near center of mound	Chimney with outer wall of anhydrite intergrown with minor pyrite; inner wall lined by chalcopyrite	10	35	<1	55	anhydrite
ALV2181-1	Fragment of 10 m high black smoker chimney complex (363±3°C) near center of mound	Chimney with outer wall of anhydrite intergrown with minor pyrite; inner wall lined by chalcopyrite	25	25	<1	50	anhydrite
ALV2183-4	Sphalerite-rich sample from the surface of the mound near white smoker complex	Massive, porous, dendritic sphalerite with minor pyrite, marcasite, and chalcopyrite	15	-	80	<5	am. silica
ALV2183-6	Massive sulfide talus with crust of Fe-oxides and atacamite from north slope of mound	Massive and colloform pyrite, partially replaced by later chalcopyrite; with minor sphalerite	75	5	10	10	am. silica
ALV2183-9	Pyrite-chalcopyrite-rich sample from the surface of the mound east of black smokers	Block of massive, colloform to dendritic pyrite with a core of massive chalcopyrite; with late am. silica	30	50	<1	20	am. silica
ALV2187-1	Bulbous, sphalerite-rich white smoker chimney (260-300°C) from white smokers	Porous, dendritic and colloform sphalerite with minor pyrite, marcasite, chalcopyrite and late am. silica	10	<2	80	10	am. silica
ALV2189-5	Massive sulfide talus with crust of Fe-oxides and atacamite from north slope of mound	Massive and colloform pyrite, partially replaced by minor amounts of late chalcopyrite	85	3	<1	10	am. silica
ALV2190-7	Pyrite-chalcopyrite-rich sample from the north slope of the mound	Massive, coarse-grained pyrite intergrown with chalcopyrite; minor sphalerite and late am. silica	40	45	<1	15	am. silica
ALV2190-8	Block of massive anhydrite with minor sulfides from the base of the black smokers	Massive, coarse-grained anhydrite with disseminated aggregates of pyrite and chalcopyrite	50	10	<1	40	anhydrite
ALV2190-11	Sphalerite-rich sample from the surface of the mound near white smoker complex	Massive, porous, dendritic sphalerite with minor pyrite, marcasite, and chalcopyrite	15	<2	75	10	am. silica
ALV2190-13	Massive pyrite-sphalerite sample from surface of mound west of black smoker complex	Massive, colloform pyrite+chalcopyrite with abundant sphalerite and late am. silica filling cavities	50	<2	30	20	am. silica
ALV2190-14	Bulbous, sphalerite-rich white smoker chimney (260-300°C) from white smoker complex	Porous, dendritic and colloform sphalerite with minor pyrite, marcasite, chalcopyrite and late am. silica	5	<2	85	10	am. silica

py = pyrite ±marcasite, ccp = chalcopyrite, sp = sphalerite, am. = amorphous

←

FIG. 5. Mineralogy and textures of massive sulfides recovered from the relict MIR Mound. (a) Massive, coarse-grained chalcopyrite–pyrite assemblage with disseminated pyrite euhedra. (b) Two-cm-wide vein of sphalerite and pyrite cutting earlier massive sulfides. No visible gold is present in the massive pyrite–chalcopyrite, and bulk gold contents are only 2.5 ppm Au (MIR–3–76–6A). However, abundant free gold occurs at concentrations up to 15.5 ppm Au (MIR–3–76–6B) in the sphalerite vein. (c) Coarse-grained euhedral pyrite in massive pyrite–chalcopyrite from the MIR Mound. (d) Sphalerite filling vein in massive pyrite–chalcopyrite, with minor late pyrite occupying open spaces.

TABLE 2. DESCRIPTION OF SELECTED SULFIDE SAMPLES RECOVERED FROM THE MIR MOUND

Sample No.	Sample Type	Description	Mineralogy (modal abundances)				
			py	ccp	sp	other	
MIR-3-76-3	Massive sulfide talus with crusts of atacamite; from western margin of mound	Massive, fine-grained, dendritic and colloform pyrite±marcasite, partially replaced by late-stage chalcopyrite	20	70	<1	<10	am. silica
MIR-3-76-5	Chimney fragments from a field of small (≤2 m high) inactive chimneys at the western edge of the main chimney field	Massive, fine-grained, dendritic and colloform pyrite±marcasite with abundant sphalerite; fluid conduits lined by sphalerite and minor euhedral chalcopyrite	60	10	25	5	am. silica
MIR-3-76-6	Sample from tall (5 m high) inactive spire, with red and yellow Fe-oxide coating; from the central part of the main chimney field	Coarse-grained, recrystallized, massive chalcopyrite with relict colloform pyrite ±marcasite; cut by 3-4 cm late vein of massive sphalerite and pyrite	35	40	20	5	am. silica
MIR-3-76-8	Samples from tall (5 m high) inactive spire, with red and yellow Fe-oxide coating; from the central part of the main chimney field	Massive, fine-grained, dendritic and colloform pyrite±marcasite with colloform sphalerite; fluid conduits lined by coarse-grained chalcopyrite	30	50	10	10	am. silica
MIR-3-76-9	Massive sulfide talus with crusts of red-brown Fe-oxides and atacamite; from the northern edge of the main chimney field	Massive, colloform pyrite±marcasite partially replaced by late-stage chalcopyrite	35	65	<1	-	
MIR-3-76-10	Massive sulfide talus from the northern edge of the main chimney field	Massive chalcopyrite replacing colloform pyrite ±marcasite; relict colloform pyrite occurs as coarse, recrystallized remnants within massive chalcopyrite	10	85	<1	<5	am. silica

py = pyrite ±marcasite, ccp = chalcopyrite, sp = sphalerite, am. = amorphous

A description of the analytical method is given by Hannington & Gorton (1991). Concentrations of Cu and Pb were determined by optical emission spectrometry (ICP–ES) in the laboratories of the Geological Survey of Canada. Specific mineral phases were analyzed by electron microprobe in wavelength-dispersion mode. Detailed mapping of the distribution of gold grains was carried out using back-scattered signals from an electron microscope transferred to an image analyzer.

A Cameca IMS–4f ion microprobe in the CANMET Laboratories in Ottawa was used to determine the "invisible" gold content of pyrite and chalcopyrite in the MIR samples. The application of SIMS to the analysis of sulfides for Au has been described in detail by Cabri & Chryssoulis (1990). Polished specimens were sputtered to depths of 0.3 to 2.0 μm with a 120 nA Cs^+ beam at 10 keV accelerating voltage. The area analyzed in each case was about 60 μm, with a maximum crater size of about 200 μm. Negative, secondary ions of ^{197}Au and ^{92}FeS were measured; ^{92}FeS was used to monitor sample homogeneity. Pyrite implanted with ^{197}Au was used as an external standard, with an implantation dose of 2.5×10^{13} ions/cm^2 at 1 MeV. Operation of the ion microprobe in high-mass-resolution mode ($M/\Delta M = 3000$) yielded minimum detection-limits below 100 ppb Au (*cf.* Larocque *et al.* 1992, 1995). Data presented in this paper are the first reported ion-microprobe results on gold content of sulfide minerals from modern seafloor deposits.

Gold in the Active TAG Mound

Samples collected from the active TAG mound resemble sulfide assemblages from deposits elsewhere on the mid-ocean ridges. The presently active, high-temperature black smokers and large blocks of massive pyrite and chalcopyrite from the surface of the mound contain high concentrations of Cu, Co, and Se, whereas lower-temperature white smokers and pyrite–sphalerite assemblages are enriched in Zn, Cd, Ag, As, and Sb (Table 3). The strong fractionation of Cu-rich and Zn-rich sulfides between the black smoker and white smoker complexes likely reflects a strong zonation of metals within the mound. Individual samples from white smoker chimneys commonly have bulk Zn contents of 50–60 wt.%, with up to 12.5 wt.% SiO_2. Gold is strongly partitioned into the lower-temperature Zn-rich portions of the mound (Fig. 6) and, in general, there is good correlation among Au, Ag, As, Sb, and Pb (Table 3; *cf.* Hannington *et al.* 1991). In particular, statistically significant correlations with Au, at a 95% confidence level, are found for Ag ($r = 0.29$) and Sb ($r = 0.48$). However, the concentrations of these elements in the black smokers are typically close to detection limits. Figure 6 shows that virtually all of the high gold-values occur in Zn-rich sulfides and that Cu-rich samples from the mound are uniformly gold-poor by comparison. Black smokers and massive pyrite–chalcopyrite assemblages typically contain <1 ppm Au and rarely have gold concentrations greater

TABLE 3. CHEMICAL COMPOSITION OF 1990 ALVIN SAMPLES FROM THE TAG HYDROTHERMAL MOUND

Sample No.		(wt%) Cu	Fe	Zn	(ppm) Au	Ag	As	Sb	Pb	Co	Se	Mo	Cd
2179-1-1A	pyrite-chalcopyrite	2.5	44.2	0.93	0.88	<5	120	3.6	140	1190	34	150	20
2179-1-1B	pyrite-chalcopyrite	23.0	31.6	0.40	0.97	6	51	5.9	34	189	52	150	<10
2179-2-2A	black smoker	9.5	23.2	0.13	0.38	6	43	1.6	34	910	230	160	<10
2179-4	black smoker	23.5	24.3	0.01	0.05	6	1	0.1	<20	106	630	140	<10
2179-4-1-1	black smoker	10.8	13.3	0.07	0.13	6	8	0.7	<20	205	315	68	<10
2179-4-1-4	black smoker	4.0	4.8	0.01	0.03	1	1	0.1	<20	56	120	9	<10
2179-4-1A1	black smoker	11.6	13.4	0.03	0.10	3	4	0.3	<20	131	370	51	<10
2179-4-1T1	black smoker	12.1	11.2	0.01	0.05	<5	1	0.1	<20	47	390	15	<10
2181-1-1A2	pyrite-chalcopyrite	8.5	19.2	0.25	0.25	7	19	0.5	31	330	160	110	<10
2183-4-1A	white smoker	0.4	6.0	58.4	13.59	1420	65	100	350	<2	<2	45	1960
2183-4-1A	white smoker	0.4	5.7	51.3	12.77	1350	60	97	-	1	<2	43	1790
2183-4-1B	white smoker	0.5	7.3	50.6	20.75	1060	42	90	300	<2	<2	48	2000
2183-4-1C	white smoker	0.4	5.4	52.7	13.36	1920	79	93	480	<2	<2	56	1780
2183-6-2A	pyrite	1.7	36.1	6.23	1.87	170	120	15	310	41	8	120	78
2183-7OA	anhydrite	0.2	0.5	0.01	<0.01	<5	1	<0.1	22	13	10	6	<10
2183-9-1A	pyrite-chalcopyrite	17.6	30.0	0.39	1.63	79	151	37	150	20	10	62	18
2187-1-1A1	white smoker	0.6	4.2	54.0	5.15	190	52	205	440	<2	<2	55	1830
2187-1-1A1	white smoker	-	6.3	49.4	9.86	150	32	199	370	<2	<2	108	1680
2187-1-1A1	white smoker	-	3.9	50.5	4.78	190	58	199	-	<2	<2	61	1660
2187-1-1B	white smoker	0.4	8.1	40.5	2.62	180	51	145	600	<2	<2	68	1080
2187-1-1C	white smoker	1.4	3.2	54.8	42.35	180	22	304	160	<2	<2	244	2030
2187-1-1C	white smoker	-	3.4	57.2	43.71	195	-	311	-	<2	<2	248	2050
2187-1-1C	white smoker	-	3.3	-	42.82	182	16	309	-	<2	<2	240	2050
2187-1-4A	white smoker	0.6	1.3	60.4	0.34	580	91	370	820	<2	<2	<1	2260
2187-1-6A	white smoker	0.5	1.6	61.5	0.18	560	117	63	1000	1	<2	<1	950
2189-5-2A	pyrite	1.0	40.3	0.45	0.66	44	44	2.9	130	89	5	125	<10
2190-7-1A	pyrite-chalcopyrite	15.9	31.7	0.92	0.70	28	48	11	150	154	5	100	20
2190-8-1A	pyrite-anhydrite	4.1	26.2	0.03	0.10	<5	35	0.7	22	337	58	78	<10
2190-11-1A	white smoker	0.6	4.2	59.9	13.08	210	48	224	370	<2	<2	35	2190
2190-11-1A	white smoker	-	4.1	55.3	13.36	240	47	224	-	<2	<2	53	2220
2190-11-1B	white smoker	0.7	15.0	38.1	4.69	70	64	127	400	<2	<2	42	1380
2190-13-1A	pyrite-sphalerite	0.4	23.0	17.6	1.01	240	63	77	380	2	<2	37	250
2190-14-1A	white smoker	0.6	0.9	62.7	15.26	1160	90	252	800	<2	<2	70	1610
2190-14-1A	white smoker	-	1.0	56.1	14.91	1090	84	252	-	<2	<2	43	1610
2190-14-1B	white smoker	0.4	2.9	53.6	0.28	1200	105	180	800	<2	<2	50	1190
2190-14-1B	white smoker	-	3.1	50.0	0.31	1180	102	181	-	<2	<2	30	1270
2190-14-1C	white smoker	0.5	0.8	58.3	0.11	1570	153	282	1100	<2	<2	64	1810
2190-14-1D	white smoker	0.7	0.5	54.2	6.03	1240	85	320	760	<2	<2	48	1800
2190-14-1D	white smoker	-	0.7	54.0	6.00	1260	91	323	-	1	7	42	1840
2190-14-1E	white smoker	0.3	1.0	56.8	0.07	1690	137	126	1100	<2	<2	16	930
2190-14-1F	white smoker	0.6	1.1	58.1	3.18	1300	89	266	550	1	<2	42	1680

'-' not analyzed

than the deposit average.

White smokers from the active mound have gold contents attaining a maximum of 42.4 ppm Au in individual subsamples. These are among the most gold-rich hydrothermal precipitates yet recovered from the seafloor. The average gold content of samples from white smoker chimneys is 9.5 ppm Au, with a median value of 6.0 ppm Au (n = 15). The gold is concentrated within the porous, delicate network of fine-grained, dendritic sphalerite that comprises the bulk of the chimneys. The sphalerite in the white smokers is distinctly iron-poor (<0.7 mol.% FeS: Fig. 7) and appears clear or white in transmitted light (Figs. 4b, c). In some samples, Ag also is highly enriched (*e.g.*, up to 0.2 wt.% in 2183–4–1), and several of the gold-rich white smokers contain traces of sulfosalt minerals, which contribute to the high levels of As, Sb, and Pb. However, the correlation between gold and silver at the scale of individual chimneys is commonly poor. Analyses of subsamples from two

TABLE 4. CHEMICAL COMPOSITION OF 1990 MIR SAMPLES FROM THE RELICT MIR MOUND

Sample No.		(wt%) Cu	Fe	Zn	(ppm) Au	Ag	As	Sb	Pb	Co	Se	Mo	Cd
MIR-3-76-3A	chalcopyrite-pyrite	29.6	26.6	<0.1	6.42	40	20	7	27	12	<2	140	<5
MIR-3-76-3B	chalcopyrite-pyrite	26.0	33.5	<0.1	6.44	10	75	5	29	15	<2	230	<5
MIR-3-76-3C	chalcopyrite-pyrite	18.4	31.2	<0.1	8.27	40	90	5	20	12	10	140	<5
MIR-3-76-5A	pyrite-sphalerite	0.5	28.0	22.9	12.94	240	180	40	510	7	<2	70	840
MIR-3-76-5B	pyrite-sphalerite	4.7	30.7	11.0	7.68	150	210	25	26	12	<2	130	450
MIR-3-76-6A	pyrite-chalcopyrite	18.3	35.4	0.8	2.52	30	100	10	26	10	<2	80	10
MIR-3-76-6B	pyrite-sphalerite vein	10.7	24.2	22.0	14.53	110	190	60	<20	12	<2	40	1050
MIR-3-76-8A	chalcopyrite-sphalerite	26.9	29.8	3.2	9.12	100	100	20	<20	11	<2	140	90
MIR-3-76-8B	chalcopyrite-sphalerite	18.5	31.1	6.6	15.51	140	150	30	44	12	2	110	230
MIR-3-76-8C	chalcopyrite-sphalerite	10.6	33.0	7.0	8.96	170	170	30	40	9	2	70	270
MIR-3-76-9A	chalcopyrite-pyrite	20.0	35.1	0.4	3.31	30	170	5	31	10	2	210	10
MIR-3-76-9B	chalcopyrite-pyrite	23.7	32.4	0.2	2.35	20	130	4	24	14	<2	230	10
MIR-3-76-10	chalcopyrite-pyrite	28.4	29.9	<0.1	0.75	40	10	4	140	13	<2	130	5

intact white smokers indicate that gold is concentrated close to fluid conduits or cavities within the chimney structures (Fig. 8). Although the bulk mineralogy does not vary significantly across the chimney walls, trace elements such as Ag, As, and Sb appear to occur in distinct zones. High concentrations of Sb occur with high Au at the center of the chimneys, and higher values of As and Ag occur at the outer margin. Nearly identical zonation was documented in similar gold-rich white smoker chimneys from the Lau Basin (Herzig *et al.* 1993) and is likely related to porosity–permeability differences, which control fluid flow through the chimney walls.

Despite the very high concentrations of gold in some

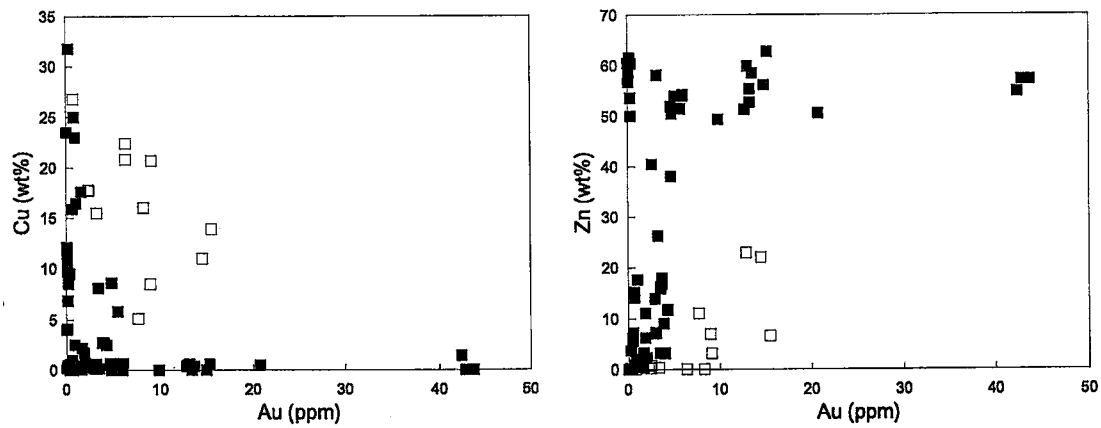

FIG. 6. Plots of Au *versus* Cu and Au *versus* Zn in bulk samples from the active TAG Mound (closed symbols) and inactive MIR Mound (open symbols). The greatest enrichment of gold at TAG is consistently found in Zn-rich chimneys, reflecting the strong fractionation of metals within the mound. A one-way correlation between Au and Zn is evident; high Au is almost always associated with high Zn, but Zn-rich samples do not always contain high gold. Exceptionally gold-rich samples are from the white smoker ALV2187–1–1. Coarse-grained, recrystallized sulfides from the MIR Mound display a separate trend of high concentrations of gold and a much narrower range of Cu and Zn contents. Data for the TAG Mound include analyses of 27 samples from Hannington *et al.* (1991) and 32 analyses from this study (Table 3). Data for the MIR Mound are from Table 4.

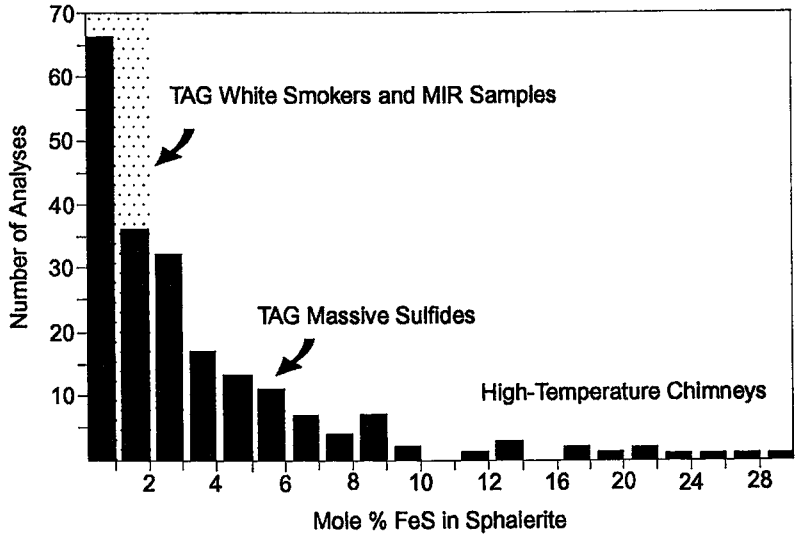

FIG. 7. Compositions of sphalerite in sulfide samples from the active TAG Mound and relict MIR Mound. Sphalerite from gold-rich white smokers on the active TAG Mound and in gold-bearing, massive sulfides from the relict MIR Mound are both distinctly iron-poor.

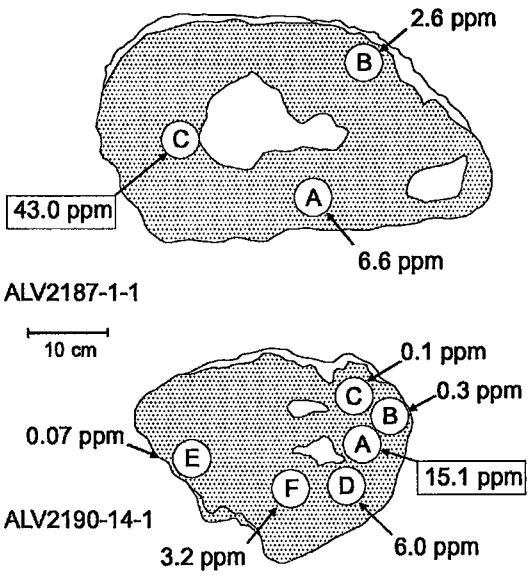

FIG. 8. Schematic horizontal cross-sections of two white smoker chimneys from the active TAG mound showing the distribution of gold in different zones: porous, massive sphalerite (shaded) and open fluid conduits (white). Gold is concentrated around the central orifice of each chimney and close to secondary fluid conduits or cavities.

samples, a discrete gold-bearing phase was not observed under the electron microscope at magnifications of up to 3,000×. This suggests that the gold is most likely present as submicroscopic particles (so-called "invisible" gold), either trapped within the fine-grained aggregates of sphalerite or adsorbed onto mineral surfaces, or in solid solution within the sulfides.

GOLD IN THE RELICT MIR MOUND

Sulfide samples recovered from the MIR mound consist of (1) massive, recrystallized chalcopyrite – pyrite – sphalerite assemblages and (2) massive pyrite – sphalerite assemblages containing relict colloform textures. Most of the MIR samples are both Cu-rich and Zn-rich (Table 4), with combined metal contents of nearly 60 wt.% Cu, Fe, and Zn. This contrasts with sulfide chimneys forming at active vents, which typically contain abundant $CaSO_4$, $BaSO_4$, or SiO_2, and less than 40% combined metals (Hannington *et al.* 1991). The high grades of Cu and Zn in samples from the MIR Mound are due, in part, to leaching of the non-sulfide phases during hydrothermal recrystallization (Rona *et al.* 1993a, b). As a result, bulk samples from the MIR Mound are chemically much more homogeneous than individual sulfide chimneys from vent complexes on the active mound. Widespread overprinting of early pyrite- and sphalerite-rich assemblages by later chalcopyrite also contributes to the high total metal contents.

Gold concentrations in the MIR samples reach 15.5 ppm Au, with an average for 13 subsamples of 7.6 ppm Au and a median value of 7.7 ppm. The gold tends to be concentrated in the highest-grade assemblages and shows a weak correlation with both Cu and Zn (Fig. 6). Samples containing the most sphalerite have the highest concentrations of gold, but concentrations of Ag, As, Sb, and Pb are generally low and resemble those of Cu-rich chimneys from the active mound (Table 4). The low concentrations of trace metals, particularly in the coarse-grained recrystallized samples, may reflect long-term hydrothermal reworking during which these elements are progressively stripped from the sulfides and remobilized to active vents on the surface of the deposit. Co and Se are close to detection limits in the MIR samples, and also may have been removed from the sulfides during hydrothermal recrystallization, as suggested for similar deposits elsewhere on the mid-ocean ridges (Hekinian & Fouquet 1985). In contrast to active chimneys on the TAG Mound, the high concentrations of gold in the MIR samples do not show a preferred correlation with any other elements, and this is consistent with the relatively late introduction of gold.

Abundant grains of native gold occur locally in gold-rich samples from the MIR Mound. The gold occupies open spaces in the coarse-grained recrystallized sulfides and also occurs along grain boundaries or within late microfractures (Fig. 9). Most of the gold occurs as irregular grains or flakes, locally with straight crystallographic boundaries and commonly in more complicated forms. These textures are consistent with the uninhibited growth of the gold grains into open spaces remaining in the coarse, recrystallized sulfides. The largest grains are up to 4 μm in diameter and are clearly visible under the reflecting microscope at only a few hundred times magnification. A total of 132 grains of gold were identified in polished specimens of a late sphalerite–pyrite vein that cuts earlier massive pyrite–chalcopyrite (MIR–3–76–6B: see Fig. 5b). The

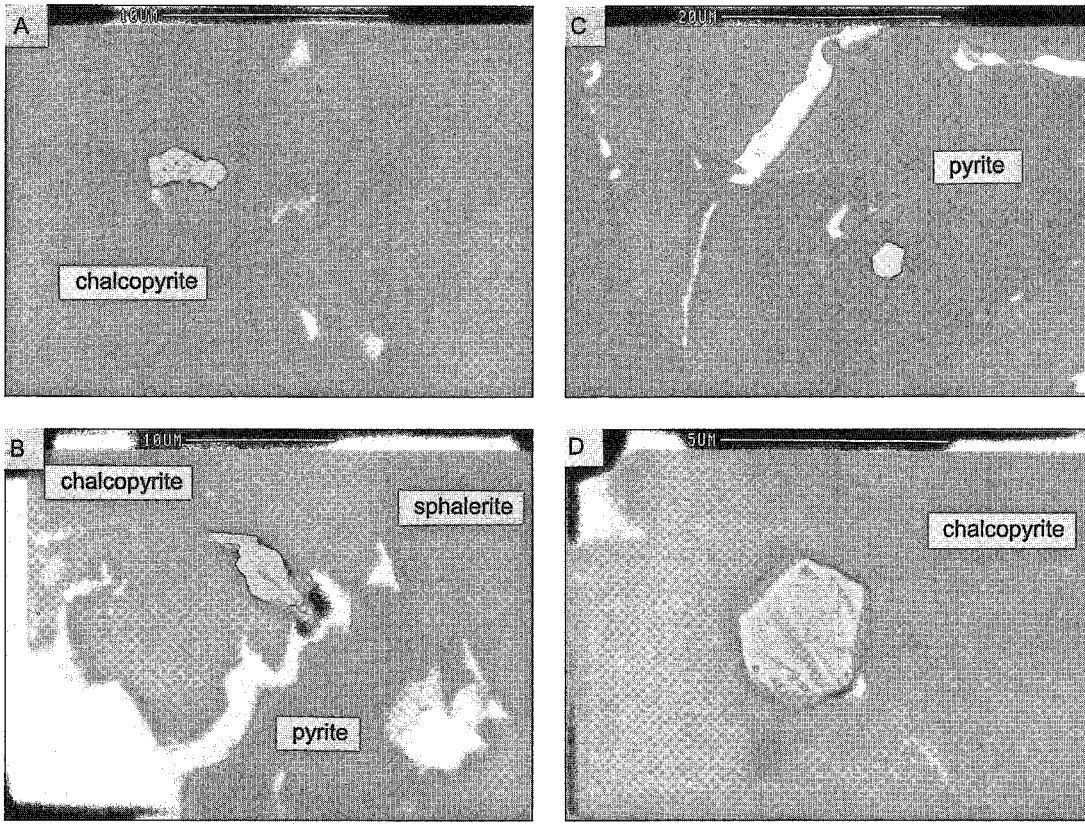

FIG. 9. SEM images of native gold in coarse, recrystallized sulfides from the MIR Mound. (a) Fine-grained gold as an inclusion within pitted chalcopyrite. (b) Coarse, 10-μm grain of gold occupying an open fracture within pyrite. (c) Equant grain of gold at the boundary between recrystallized pyrite and chalcopyrite. (d) Close-up of gold grain in (c). Note that most of the gold is found as late grains, (1) filling open spaces (2) within chalcopyrite and recrystallized pyrite, and (3) at grain boundaries and in open spaces within massive pyrite–sphalerite and late cross-cutting microveinlets.

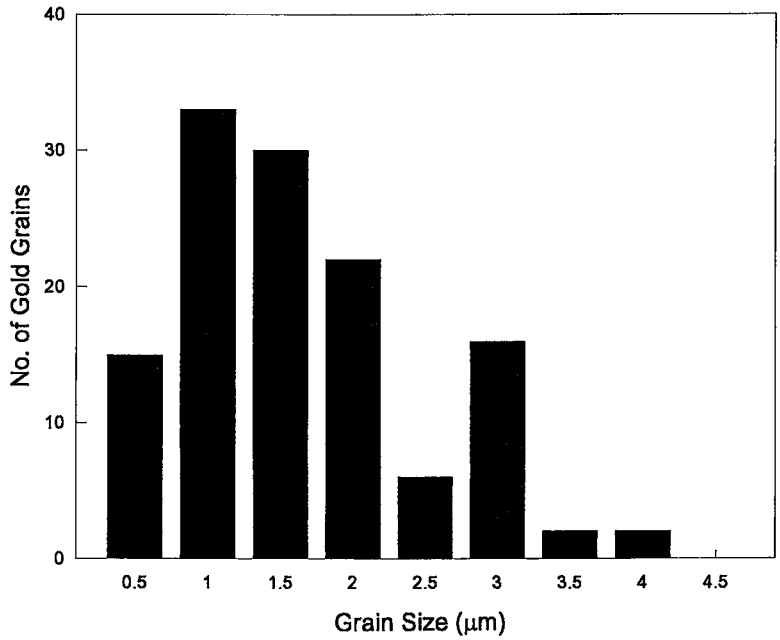

FIG. 10. Grain-size distribution of native gold in MIR–3–76–6B. Grain-size analysis was performed by means of an image analyzer interfaced with the SEM. In all, 132 grains of gold were identified, with 50% <1 μm in diameter and 80% ≤2 μm. The largest grain observed in polished specimens was only 4 μm in diameter.

gold in the vein is visible at magnifications of about 3,000–10,000×, with 80% of the grains smaller than 2 μm and 50% less than 1 μm in diameter (Fig. 10). Although the number of large grains (>2 μm) is small, they account for 72% of the total mass of gold, and a single 4-μm grain out of 132 grains accounts for nearly 10% of the total gold in the sample. Electron-microprobe analyses of the MIR samples for Au indicate that it is of uniformly high purity. All of the gold grains analyzed contain less than about 5 wt.% Ag (fineness ≥950: Fig. 11, Table 5), and no zonation was found in the Au/Ag ratio within individual grains. This contrasts with the gold in many ancient massive sulfide deposits, in which the principal gold-bearing phase is electrum (*e.g.*, >20 wt.% Ag).

The coarse grain-size of recrystallized sulfides in the MIR Mound permits direct analysis of individual minerals by ion-microprobe techniques. Fifteen analyses of pyrite and chalcopyrite in four samples

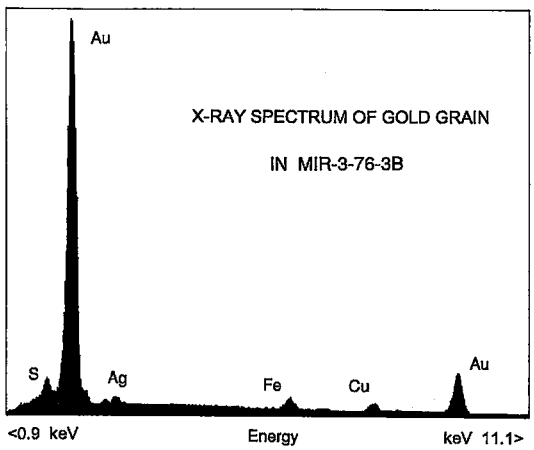

FIG. 11. X-ray spectrum of typical gold grain in MIR–3–76–6B.

TABLE 5. ELECTRON MICROPROBE DATA ON GOLD IN MIR-3-76-6B

Au (wt%)	96.8	98.7	92.1	95.6	92.4	94.7	93.3	98.9
Ag	4.7	3.8	3.0	5.2	5.9	5.0	3.9	3.9
	101.5	102.5	95.1	100.8	98.3	99.7	97.2	102.8
Fineness	953	962	968	948	940	950	960	962

TABLE 6. CONCENTRATION OF Au IN PYRITE AND CHALCOPYRITE FROM MIR SAMPLES, AS DETERMINED BY SIMS

Sample	Mineral	Analysis Points (ppm Au)		
MIR-3-76-6A	pyrite	0.8	2.0	0.9
MIR-3-76-6A	chalcopyrite	<0.05	0.1	0.1
MIR-3-76-3A	chalcopyrite	1.0	0.4	0.8
MIR-3-76-3B	chalcopyrite	0.5	0.5	0.7
MIR-3-76-8-3	chalcopyrite	0.3	0.08	1.0

indicate that a small fraction of the bulk gold in some of the MIR sulfides is present as "invisible" gold, either incorporated in the sulfides during recrystallization or as a residue of submicroscopic gold precipitated with the sulfides earlier in their history. Analyses of individual grains of pyrite and chalcopyrite to a depth of 2 μm reveal minor amounts of submicroscopic gold (particles <0.2 μm in size) at concentrations ranging from <0.05 up to 2 ppm Au (Table 6). Figure 12 shows a depth profile to 0.4 μm in pyrite from sample MIR–3–76–6A. The variation in gold concentration with the depth of penetration is relatively flat in the lower portion of the profile, suggesting that the gold is homogeneously distributed through this part of the sample at a concentration of <1 ppm Au. However, a broad peak from the surface of the sample to a depth of 0.2 μm may be due to the presence of dispersed, colloid-sized particles of gold at concentrations up to 2 ppm Au. The background concentrations of Au in pyrite and chalcopyrite from these samples are close to the bulk gold contents of typical black smoker chimneys (*e.g.*, Hannington *et al.* 1991) and are similar to the concentrations of invisible gold typically found in pyrite and chalcopyrite from ancient massive sulfide deposits (*e.g.*, Chryssoulis *et al.* 1989, Cook & Chryssoulis 1990). Although the number of ion-probe analyses is not statistically significant, the low background concentrations of gold in these samples are consistent with only a small fraction of the total gold content of the samples being present as "invisible" gold. An accounting of the gold distribution in each of these samples indicates that less than 10% of the total occurs as submicroscopic inclusions or invisible gold locked in pyrite and chalcopyrite.

Physical and Chemical Controls on the Occurrence of Gold

The distribution of gold in sulfide samples from the active mound (*i.e.*, high levels of Au in the white smoker complex and relatively low levels in black smokers) reflects the strong thermal and chemical gradients surrounding the main upflow zone. Low-temperature, white smokers at the cool outer margins of the upflow zone contain most of the Zn and virtually all of

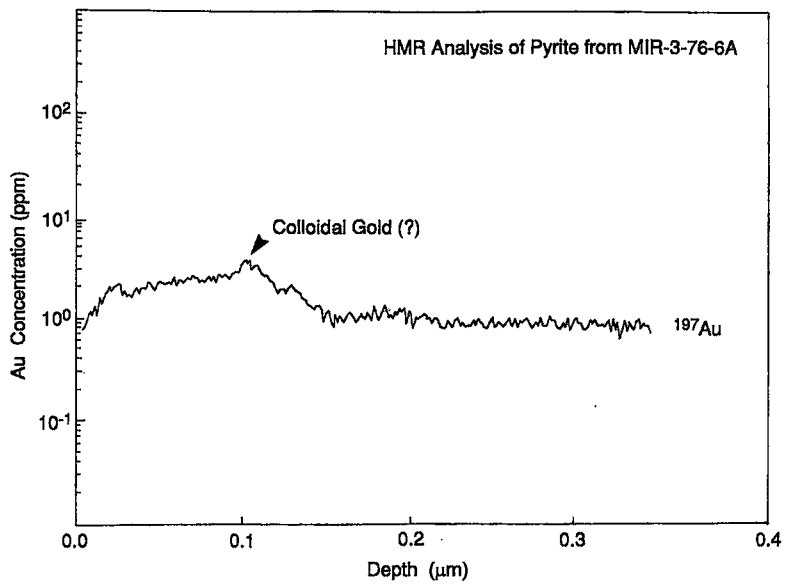

FIG. 12. Depth profile of gold concentrations in pyrite from MIR–3–76–6A using the Cameca IMS–4f ion microprobe. Analysis of the pyrite reveals background concentrations of about 1 ppm Au (submicroscopic particles <0.2 μm) and possible inclusions of colloidal gold at concentrations of up to 2 ppm Au.

the gold, and this is interpreted to reflect both the strong temperature-dependence of gold transport through the mound and the efficiency of gold deposition within the white smoker chimneys. As fluids are transported away from the central upflow zone, cooling and deposition of sulfides contribute to the effective precipitation of gold, both in low-temperature white smoker chimneys and in sphalerite-rich veins leading to vents at the surface. For example, the gold-rich sphalerite vein observed in MIR–3–76–3B may have been a low-temperature feeder for white smoker chimneys once present on the MIR Mound. The sphalerite in this vein is notably Fe-poor (<2 mol % FeS) and consistent with this feature having been a conduit for low-temperature white smokers similar to those on the presently active TAG Mound. In contrast, fluids discharged directly through the central black smoker complex are vented before they can cool substantially below the temperature of gold saturation (*e.g.*, Hannington & Scott 1989a). As a result, much of the gold and other soluble phases in the black smoker fluids is lost to the hydrothermal plume.

Previous modeling of fluid chemistry from mid-ocean-ridge vent sites indicates that gold transport is due largely to aqueous complexes of sulfur and that precipitation of the gold is most likely to be caused by oxidation of $Au(HS)_2^-$ during mixing at relatively low temperatures (Hannington & Scott 1989a). However, in the absence of an identifiable gold-bearing mineral with known solubility in many of the gold-rich seafloor sulfides, it was difficult to prove that local enrichment of gold was a consequence of saturation of the vent fluids and direct precipitation from solution (Hannington & Scott 1989a). The abundant microscopic gold in samples from the MIR Mound confirms that gold was being precipitated directly from solution as the native metal and not simply incorporated as a trace element in other phases.

In a large, complex hydrothermal system such as the TAG Mound, the variable concentrations of gold in different sulfide assemblages arise from the different mixing–cooling histories of black smoker and white smoker fluids. Sulfides that precipitate at depth in the mound are likely to be gold-poor because of the relatively high temperatures and the strong redox buffering capacity of the fluids, which inhibits oxidation of $Au(HS)_2^-$ (Fig. 13). At white smoker temperatures, the redox buffer capacity of the fluids is gradually exhausted by the precipitation of reduced components from solution, and the vent fluid – seawater mixture approaches the H_2S–HSO_4^- boundary (Fig. 13). Under these conditions, a relatively small increment of oxida-

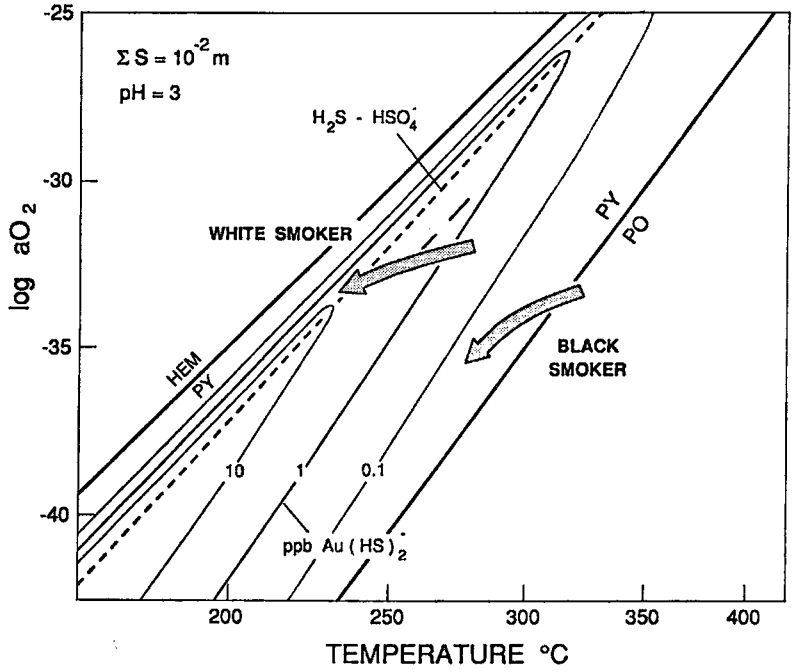

FIG. 13. Chemical evolution of black smokers and white smokers in the TAG Hydrothermal Field, showing the precipitation of gold from typical white smoker fluids as a result of cooling and increasing aO_2 during mixing with seawater (modified from Hannington & Scott 1989a).

tion may be sufficient to precipitate the gold. This latter process could be particularly important in the porous interiors of white smoker chimneys because the diffuse nature of venting allows for efficient mixing with seawater and enhanced cooling and oxidation. Because the precipitation of gold in the white smokers is a cumulative process, significant concentrations of gold in the sulfides can result from very low concentrations of gold in solution. Herzig *et al.* (1993) attributed similar high gold contents in white smoker chimneys from the Lau Basin to the effective precipitation of gold metal caused by mixing and cooling within the porous walls of the chimneys.

In several of the black smokers on the TAG Mound, the presence of an assemblage of pyrite, chalcopyrite, and bornite implies a relatively high aO_2 at high temperatures. Detailed thermal–chemical studies of the fluid compositions from black smokers at TAG indicate that some vents are close to equilibrium with pyrite–hematite at 290–320°C (Tivey *et al.* 1995), consistent with an oxidation state orders of magnitude higher than in typical mid-ocean ridge black smokers. Under these conditions, such fluids may become saturated with gold as $Au(HS)_2^-$ at relatively high temperatures (Fig. 13), leading to the early precipitation of gold in some Cu-rich assemblages. This may account for local enrichment of up to 2 ppm Au observed in several Cu-rich chimneys from the black smoker complex (Hannington *et al.* 1989a) and similar elevated gold contents in black smokers containing bornite + pyrite in the Snakepit hydrothermal field (Fouquet *et al.* 1993).

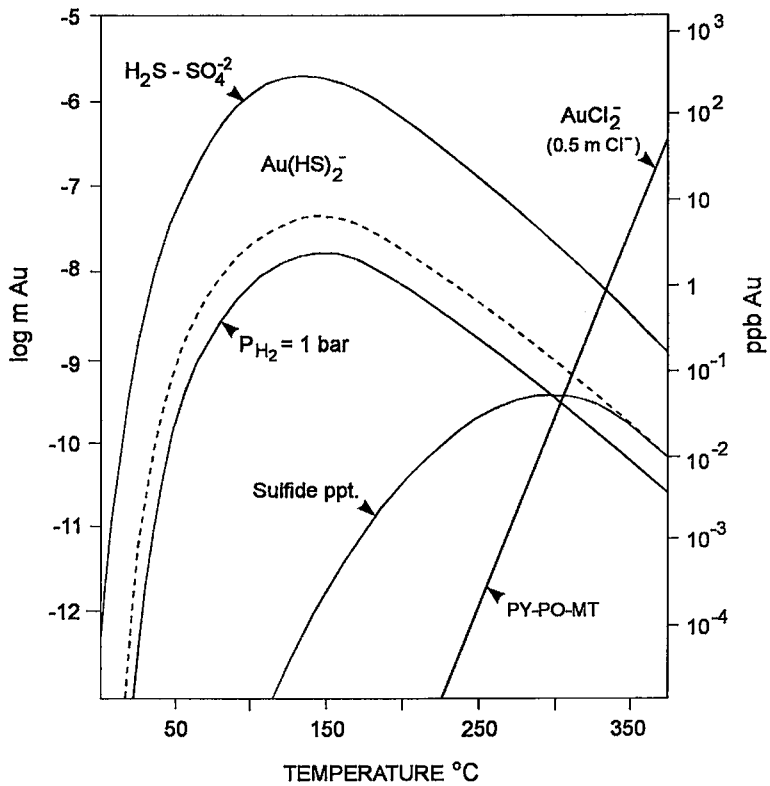

FIG. 14. Hypothetical curves of gold solubility showing the maximum concentrations of $Au(HS)_2^-$ for different sulfide–oxide buffers. Temperature, pH, and H_2S concentrations are modeled as a function of linear mixing between ambient seawater and a 350°C end-member fluid with a starting composition of pH = 3.5 and log m H_2S = –2.2. The upper limit of aO_2 conditions measured in typical seafloor hydrothermal vents is indicated by the dashed line (PH_2 = 0.1 bar). Gold solubilities for H_2S–SO_4^{2-} equilibrium and PH_2 = 1 bar are calculated for mixing without sulfide precipitation (H_2S is conserved). The lowermost curve is for mixing with sulfide precipitation; decreasing concentrations of H_2S with temperature are approximated by the solubility of pyrite – pyrrhotite – magnetite (Crerar *et al.* 1978). The calculated solubility maxima for $Au(HS)_2^-$ fall between 300 and 150°C and correspond to the range of vent temperatures for typical white smoker chimneys. Equilibrium constants for $Au(HS)_2^-$ are from Seward (1976), Shenberger & Barnes (1989), and Renders & Seward (1989a). The solubility of gold as $AuCl_2^-$ is calculated on the pyrite – pyrrhotite – magnetite buffer for m Cl^- = 0.5; data for $AuCl_2^-$ are from Helgeson (1969).

TABLE 7. COMPOSITION OF VENT FLUIDS FROM THE TAG MOUND

	Black Smokers	White Smokers
T°C	360–366	265–300
pH (in situ)	4.4	3.8
H_2S mM	2.5–3.5	0.5
Fe ppm	312	183–212
Cu	8–10	<0.2
Zn	3	16–26

Sources: Edmond et al. (1990), Edmond et al. (1995), Tivey et al. (1995).

For the most part, however, high concentrations of gold in the white smoker chimneys reflect the strong tendency for $Au(HS)_2^-$ to remain in solution down to quite low temperatures. This is illustrated in Figure 14, which shows hypothetical curves of gold solubility for different sulfide–oxide buffers. The calculated solubility maxima for gold under conditions of modern seafloor vents fall between 300°C and 100°C and correspond to the range of vent temperatures for typical white smokers. In modern seafloor vents, the concentrations of gold in high-temperature, end-member solutions are on the order of 0.1 ppb Au (Campbell *et al.* 1987, Hannington & Scott 1989a, Falkner & Edmond 1990). Depending on the redox buffer, these fluids may become saturated with gold only at very low temperatures, where the solubility of the native metal drops below 0.1 ppb Au. However, the precipitation of gold at white smoker temperatures may be significantly enhanced by a large decrease in the concentration of H_2S in solution as a result of oxidation or precipitation of sulfides. This effect is illustrated by the lowermost curve in Figure 14. A comparison of vent fluid compositions from the white smoker complex and the nearby black smoker vents (Table 7) indicates a sharp decrease in H_2S concentration with temperature, together with lower pH and distinctly lower Cu and Fe concentrations, consistent with the precipitation of sulfides as a result of cooling within the mound (Edmond *et al.* 1990, 1995, Tivey *et al.* 1995). The large decrease in H_2S prior to venting may contribute to the effective precipitation of gold from $Au(HS)_2^-$ at white smoker temperatures and may cause the deposition of gold beneath the vent complex (*e.g.*, in sphalerite-rich veins similar to those found on the MIR Mound).

The association of gold with low-Fe sphalerite in both the active and relict sulfide mounds at TAG supports earlier indications of a similar relationship in other deposits (Hannington & Scott 1989b). The correlation between bulk gold contents and the composition of coexisting sphalerite was explained in terms of the activity of sulfur in the hydrothermal fluid, which relates to both the solubility of gold as an aqueous sulfur complex and the iron content of sphalerite. New data from the TAG Hydrothermal Field apparently extend this observed trend to very low Fe contents in sphalerite and very high concentrations of gold (Fig. 15).

The porous matrix of dendritic sphalerite that fills the white smoker chimneys (*e.g.*, Fig. 4) may be particularly suitable for the deposition of gold. The dendritic sphalerite is formed by rapid quenching and turbulent flow of the hydrothermal fluids as they enter the chimney structure, but complex channelways through the sphalerite matrix eventually impede the flow of fluid, resulting in more diffuse venting and creation of a potential trap for gold. The longer residence-time and relatively low temperatures of the hydrothermal fluids within the white smokers and the large surface-area provided by the dendritic sphalerite will significantly enhance the precipitation of gold from solution and may also contribute to adsorption of gold and other trace metals onto exposed sulfide surfaces. This latter process has been widely suggested as a possible means of concentrating gold

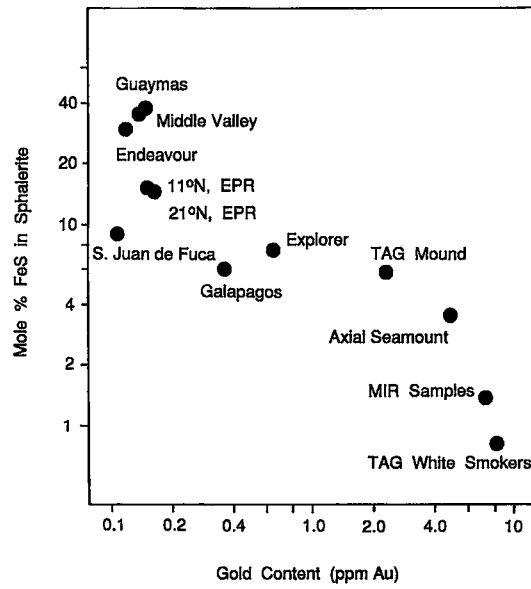

FIG. 15. Log–log plot of average sphalerite compositions *versus* average gold contents for modern seafloor sulfides (modified from Hannington & Scott 1989b). New data from the TAG Hydrothermal Field extends this relationship to much higher concentrations of gold. Data ranges and standard deviations for each deposit are given by Hannington & Scott (1989b).

and associated trace elements from hydrothermal solutions, independent of their saturation state (Bancroft & Jean 1982, Seward 1984, Jean & Bancroft 1985, Krupp & Seward 1987, Renders & Seward 1989b). The common association of gold with fine-grained sulfosalts in some low-temperature white smokers suggests that these phases may be important sites for the codeposition or adsorption of gold (*e.g.*, Zierenberg & Schiffman 1990, Hannington *et al.* 1991, Fouquet *et al.* 1993), as observed in many active geothermal systems on land. For example, Krupp & Seward (1987) noted that gold associated with high concentrations of Ag, As, and especially Sb in some New Zealand hot springs may have been concentrated from solutions by adsorption onto amorphous sulfide phases. Despite concentrations of up to 50 ppm Au in the hot-spring sinters, the gold does not appear to have crystallized as a discrete mineral phase. A similar process could explain the absence of identifiable minerals of gold in gold-rich white smokers on the TAG Mound. Further detailed work is required to determine exactly how the gold occurs in these white smoker chimneys.

Although gold-rich white smokers at the surface of the TAG Mound are locally enriched in Ag (up to 0.1 wt.%), the bulk Au/Ag ratios of the TAG sulfides span nearly four orders of magnitude (Fig. 16). Gold and silver are closely associated on the deposit scale (*e.g.*, in the white smoker complex), but not at the scale of individual chimneys and not at all in the recrystallized sulfides of the MIR Mound. The Au/Ag ratio in end-member hydrothermal fluids is about 0.02–0.03, based on measured concentrations of about 4 ppb Ag (Von Damm *et al.* 1985) and a gold content of about 0.1 ppb Au. This value is fairly high in comparison to other geothermal fluids and likely reflects the high Au/Ag ratio of the basaltic source-rocks (Hannington *et al.* 1986, Hannington & Scott 1989a). Black smoker chimneys on the TAG Mound have bulk Au/Ag values between 0.2 and 0.01, averaging close to that of typical end-member hydrothermal fluids. However, white smokers from the same deposit have Au/Ag ratios ranging from 0.2 to as low as 10^{-5}. Sulfides from the MIR Mound have much lower Ag contents and a much narrower range of Au/Ag ratios, close to 0.15 (0.6 to 0.02), and consistently higher than that of typical end-member fluids. Large deviations in the Au/Ag ratios of the sulfides compared to end-member hydrothermal fluids (*e.g.*, Fig. 16) imply fractionation of Au and Ag during mineralization. Unlike gold, silver is transported in vent fluids dominantly as $AgCl_2^-$, which is stable over a much larger range of temperatures than $Au(HS)_2^-$ (Seward 1976, Sugaki *et al.* 1987, Gammons & Barnes

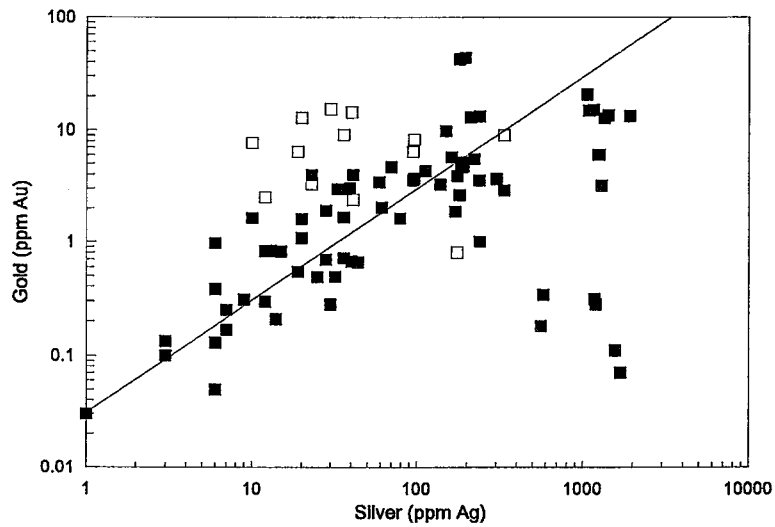

FIG. 16. Au/Ag ratios in bulk samples from the active TAG Mound (closed symbols) and inactive MIR Mound (open symbols). Samples from the MIR mound tend to have higher Au/Ag ratios, possibly reflecting the chemical refining of gold during hydrothermal reworking. The Au/Ag ratio of a typical MOR end-member hydrothermal fluid (0.02) is indicated by the diagonal line (see text for discussion). Data for the TAG Mound include analyses of 27 samples from Hannington *et al.* (1991) and 32 analyses from this study (Table 3), including nine duplicate samples. Data for 13 samples from the MIR Mound are from Table 4.

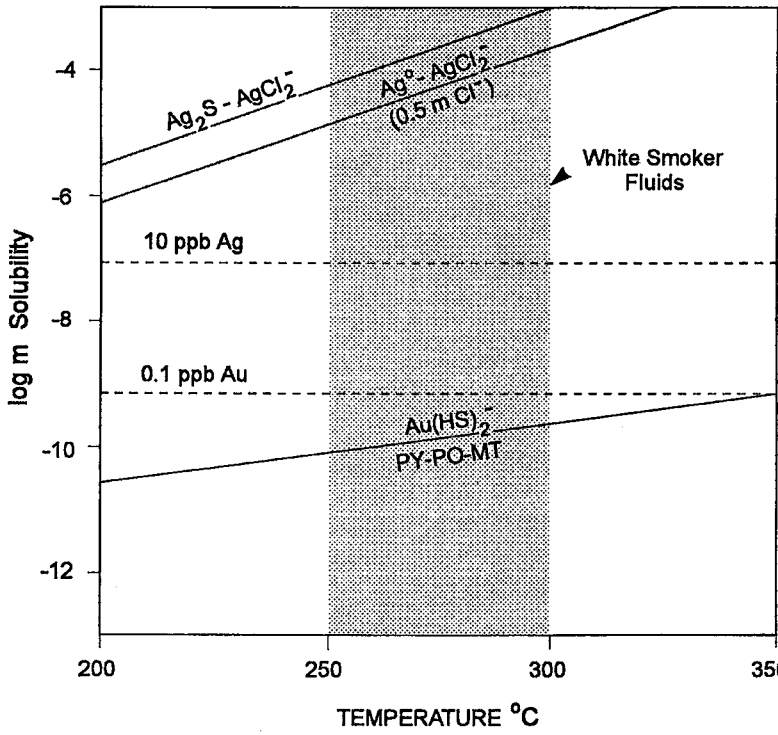

FIG. 17. Relative solubilities of gold and silver in white smoker vent fluids. Silver solubility is shown for both Ag metal and Ag_2S (*i.e.*, argentite or Ag_2S components of sulfosalt minerals). Gold solubility as $Au(HS)_2^-$ is calculated for mixing with sulfide precipitation as in Figure 15. Ag^+ chloride complexes are the principal control on silver solubility at temperatures >200°C and pH < 5, although $Ag(HS)_2^-$ complexing may be important at lower temperatures and higher pH (Seward 1976, Sugaki *et al.* 1987, Gammons & Barnes 1989). At white smoker temperatures, the fluids are close to saturation with gold, but are highly undersaturated with silver. Cooling of these fluids below white smoker temperatures may result in the effective separation of gold and silver in the hydrothermal precipitates.

1989). Most seafloor vents are significantly below saturation with respect to silver, either as silver metal or silver sulfide (*e.g.*, argentite or Ag_2S component in silver sulfosalts), and typical white smoker fluids may be 3–4 orders of magnitude undersaturated at temperatures of 250–300°C (Fig. 17). The different solubilities of gold and silver likely account for the strong zonation of these metals found in a number of gold-rich white smoker chimneys. For example, gold may be precipitated from fluids that are initially undersaturated with Ag but that become saturated at lower temperatures. This has been demonstrated in a gold-rich white smoker chimney from the Lau Basin, where gold was deposited at about 250°C in the interior of the chimney, and silver-bearing sulfides were precipitated at temperatures closer to 200°C, in the cooler outer margins (Herzig *et al.* 1993).

The different solubilities of gold and silver may also have an important impact on the compositions of electrum and gold in the sulfides. In most massive sulfide deposits, the compositions of electrum and gold mimic the bulk Au/Ag ratios of the sulfides and fall naturally into two groups: (1) high-fineness gold in Cu–Au assemblages, and (2) low-fineness electrum in polymetallic Zn–Pb–Ag assemblages (*e.g.*, Morrison *et al.* 1991, Huston *et al.* 1992, Craig & Rimstidt 1985). Morrison *et al.* (1991) summarized the relative solubilities of gold and silver in a variety of deposit types and found that, in many cases, ore fluids that are close to saturation with Au are highly undersaturated with Ag. They attributed the high fineness of gold associated with Cu-rich ores to the large degree of undersaturation of the fluids, with Ag at high temperatures and low pH. Huston *et al.* (1992) also argued that

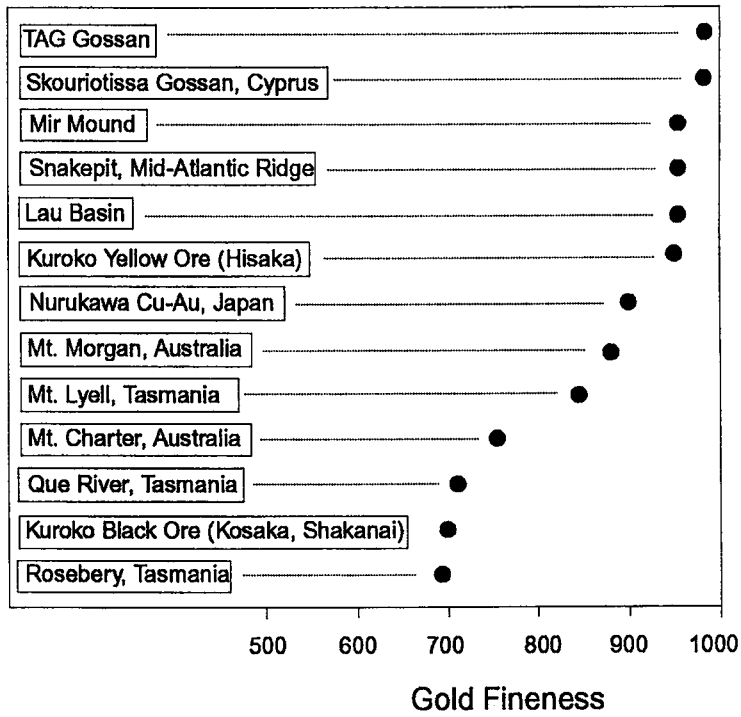

Fig. 18. Comparison of the compositions of gold and electrum in modern and ancient VMS deposits The data plotted are median values of gold fineness from Morrison *et al.* (1991), Huston *et al.* (1992), Shimazaki (1974), Herzig *et al.* (1991), Fouquet *et al.* (1993), and this study.

the association of high-purity gold with Cu-rich sulfides is a consequence of the precipitation of gold from a chloride complex ($AuCl_2^-$) at high temperatures, under conditions where Ag remains in solution. Where it has been found in modern seafloor deposits, native gold also tends to be of very high purity, resembling that of Cu–Au assemblages in ancient massive sulfides (Fig. 18). However, a convincing Cu–Au association has not been found in any of the modern seafloor sulfides, and known examples of high-purity gold occur mainly in Zn-rich assemblages. This may reflect a combination of the solubility controls on gold and silver, in which differences in their solubility persist down to a relatively low temperature, and the high Au/Ag ratio of the source fluids. Early work on the system Au–Ag–S also demonstrated that the composition of electrum in equilibrium with argentite is a strong function of temperature and aS_2 (Barton 1980), and these parameters may partly control the fineness of gold in some massive sulfide deposits. For example, the uniformly low iron contents in sphalerite from gold-rich seafloor sulfides are indicative of high-aS_2 conditions that may have contributed to the low Ag contents of associated native gold (*e.g.*, Herzig *et al.* 1993, Fouquet *et al.* 1993, this study).

Hydrothermal Reworking of Gold

Observations from the MIR Mound indicate that large sulfide deposits now forming on the modern seafloor are subject to extensive recrystallization, replacement, and chemical refining as a result of continuous hydrothermal reworking at the time of mound development. The distribution of gold in these deposits is likely to be strongly influenced by a variety of late-stage hydrothermal events. Hannington *et al.* (1986) first suggested that early-formed gold may be remobilized from massive sulfides within a mound and reconcentrated along with Zn-rich sulfides at its cooler, outer margins. This process of zone-refining was originally proposed by Hekinian *et al.* (1985) and Hekinian & Fouquet (1985) to account for the distribution of Cu- and Zn-rich chimneys on large modern seafloor deposits, following the model for Kuroko-type

deposits described by Eldridge *et al.* (1983). Although a number of large seafloor sulfide deposits with long histories of hydrothermal activity have likely experienced extensive hydrothermal reworking (*e.g.*, Hekinian & Fouquet 1985, Scott *et al.* 1990), the systematic sampling required to demonstrate this process has not previously been carried out.

Mapping of the surface of the active TAG mound has shown that the growth of the deposit is partly a result accumulating sulfide talus from the collapse of chimneys at the vent complexes (Thompson *et al.* 1988, Rona *et al.* 1993a, Tivey *et al.* 1995). The top of the mound is littered with sulfide debris, and the presently active white smoker complex is built on top of sulfide talus derived from the collapse of pre-existing chimneys. During the growth of the deposit, this sulfide debris is overgrown by later hydrothermal precipitates and gradually incorporated in the mound. Sampling at the surface of the mound indicates that gold-rich material from the collapse of white smoker chimneys is abundant in the sulfide debris. Periodically throughout their history, the deposits also may have overgrown their own sulfide gossans, incorporating secondary gold from weathered material at the surface. The flow of hydrothermal fluids through this debris results in the selective dissolution of pre-existing chimney material and remobilization of the lower-temperature constituents to the surface of the mound. The dissolution of sphalerite from within the mound is confirmed by the unusually high Zn contents of fluids currently venting from the white smoker complex (Table 7: Edmond *et al.* 1990, Tivey *et al.* 1995). Gold from auriferous white smoker debris also may be readily dissolved and ultimately reprecipitated at new white smokers on the surface of the deposit. The dissolution of gold from this older material is likely an important source of "new" gold in the presently active vents. During the life of the hydrothermal system, the continuous recycling of gold may lead to exceptionally enriched zones near the top of the deposit and progressively depleted zones at depth. Gold eventually may be stripped entirely from the sulfide mound, and in a long-lived, high-temperature system, the end-product of sustained hydrothermal reworking may be a distinctly gold-poor deposit.

In samples from the MIR Mound, there is a close association between the extent of hydrothermal recrystallization of the sulfides and the presence of microscopically visible gold. Native gold along the grain boundaries between pyrite and chalcopyrite in coarse-grained, recrystallized sulfides could have formed by the liberation of earlier submicroscopic gold during hydrothermal reworking. Similar textures in ancient massive sulfide deposits are commonly attributed to the liberation of gold from auriferous pyrite during recrystallization under conditions of high strain associated with regional metamorphism. The very high Au/Ag ratios of the sulfides from the MIR Mound also suggest that Au and Ag are separated, according to their respective solubilities, during prolonged hydrothermal reworking of the sulfides. The low abundance of Ag in recrystallized sulfides from the MIR Mound, coupled with the high concentrations of Ag in some white smoker chimneys at the surface of the active mound, suggest that Ag may be leached preferentially from the sulfides as $AgCl_2^-$ during reworking. This would contribute to progressively higher Au/Ag ratios in the recrystallized sulfides and lower Au/Ag ratios in hydrothermal precipitates forming at the surface of the mound. A similar process has been suggested to explain the high silver contents found in electrum from the upper parts of some Kuroko deposits (*e.g.*, Shimazaki 1974). The high purity of the native gold in the MIR sulfides also may reflect chemical refining that occurs during repeated dissolution and reprecipitation, a mechanism similar to that responsible for the formation of high-purity residual gold in sulfide gossans (*e.g.*, Mann 1984, Webster 1986).

Summary and Conclusions

A number of factors may have contributed to the exceptional enrichment of gold in surface samples from the TAG Hydrothermal Field, including (1) the separation of gold from other elements as fluids are transported away from the main upflow zone to the cooler, outer margins of the deposit, (2) the enhanced cooling and oxidation of vent fluids and the efficient precipitation of gold caused by diffuse venting through white smokers chimneys, (3) the concentration of gold from otherwise undersaturated solutions by adsorption onto mineral surfaces in the porous white smokers, and (4) the extensive hydrothermal reworking and reconcentration of gold from auriferous sulfide debris incorporated in the mound during earlier stages of growth. Cooling of hydrothermal fluids at the margins of the upflow zone has led to the effective separation of Cu and Zn, with most of the gold occurring in the lower-temperature, Zn-rich sulfides at the surface of the mound and locally within feeders leading to the white smoker vent complex. The high concentrations of gold in white smokers on the active TAG Mound and the presence of microscopic gold in a gold-rich sphalerite vein from the MIR Mound support this model. Sustained, low-temperature upflow at the cooler outer margins of the deposit also may lead to the dissolution of gold from older sulfides that are exposed to the rising hydrothermal solutions. The remobilization of submicroscopic gold from earlier generations of gold-rich sulfides (*e.g.*, older white smoker debris) is considered to be an important source for the local enrichment of gold in the upper parts of the TAG Mound and nearby relict MIR Mound. Repeated dissolution and reprecipitation of early-formed gold during hydrothermal reworking of the

sulfides may be responsible for the formation relatively coarse-grained, high-purity native gold now present in the MIR samples. The results of this study support the notion that gold may be continuously recycled to the upper part of the mound during its venting history and offer additional support for the zone-refining model of gold enrichment in ancient volcanogenic massive sulfides. A long history of hydrothermal reworking in the presently active TAG Mound eventually may result in the gradual depletion of gold in its interior (*i.e.*, over-refining). Recent drilling of the TAG Mound during Leg 158 of the Ocean Drilling Program (Leg 158 Scientific Party 1995) has provided new samples to test this model, and the results of this new work will be presented elsewhere.

Acknowledgements

Samples from the TAG Hydrothermal Field were collected by the authors during an *ALVIN/Atlantis II* cruise in 1990 and by Y.A. Bogdanov and P.A. Rona during a *MIR/Keldysh* cruise in 1991. We thank the officers and crew of these vessels for their assistance. The authors thank L.G.I. Bennett and K.S. Nielsen (Royal Military College of Canada) for their assistance with neutron-activation analysis. SIMS analyses were carried out with the assistance of L.J. Cabri and J.A. Jackman (CANMET). SEM photography and image analysis was performed by D. Walker in the laboratories of the GSC. Electron-microprobe analyses were conducted by I. Kjarsgaard. S.P. received support for this work from the German Ministry of Education (DAAD). An original version of the manuscript was much improved by helpful reviews from I.R. Jonasson, T.J. Barrett, S. Juras, and particularly insightful comments by R. Sherlock.

References

Bancroft, G.M. & Jean, G. (1982): Gold deposition at low temperature on sulphide minerals. *Nature* **298**, 730-731.

Barton, M.D. (1980): The Au–Ag–S system. *Econ. Geol.* **75**, 303-316.

Bluth, G. & Ohmoto, H. (1988): Sulfide–sulfate chimneys on the East Pacific Rise, 11° and 13°N latitude. II. Sulfur isotopes. *Can. Mineral.* **26**, 505-515.

Cabri, L.J. & Chryssoulis, S.L. (1990): Advanced methods of trace element microbeam analysis. *In* Advanced Microscopic Studies of Ore Minerals (J.L. Jambor & D.J. Vaughan, eds.). *Mineral. Assoc. Can., Short-Course Vol.* **17**, 341-377.

Campbell, A.C., Edmond, J.M., Colodner, D., Palmer, M.R. & Falkner, K.K. (1987): Chemistry of hydrothermal fluids from the Mariana trough back arc basin in comparison to mid-ocean ridge fluids. *Eos (Trans. Am. Geophys. Union)* **68**, 1531 (abstr.).

Chryssoulis, S.L., Cabri, L.J. & Lennard, W. (1989): Calibration of the ion microprobe for quantitative trace precious metal analysis of ore minerals. *Econ. Geol.* **84**, 1684-1689.

Constantinou, G. & Govett, G.J.S. (1972): Genesis of sulphide deposits, ochre and umber of Cyprus. *Inst. Mining Metall. Trans.* **81**, B34-B46.

_____ & _____ (1973): Geology, geochemistry, and genesis of Cyprus sulphide deposits. *Econ. Geol.* **68**, 843-858.

Cook, N.J. & Chryssoulis, S.L. (1990): Concentrations of "invisible gold" in the common sulfides. *Can. Mineral.* **28**, 1-16.

Craig, J.R. & Rimstidt, J.D. (1985): Gold: compositional variations of naturally occurring alloys. *Geol. Soc. Am., Abstr. Programs* **17**, 555.

Crerar, D.A., Susak, N.J., Borcsik, M. & Schwartz, S. (1978): Solubility of the buffer assemblage pyrite + pyrrhotite + magnetite in NaCl solutions from 200 to 350°C. *Geochim. Cosmochim. Acta* **42**, 1427-1437.

Edmond, J.M., Campbell, A.C., Palmer, M.R. & German, C.R. (1990): Geochemistry of hydrothermal fluids from the Mid-Atlantic Ridge: TAG and MARK 1990. *Eos (Trans. Am. Geophys. Union)* **71**, 1650-1651 (abstr.).

_____, _____, _____, _____, Klinkhammer, G.P., Edmonds, H.N., Elderfield, H., Thompson, G. & Rona, P. (1995): Time series studies of vent fluids from the TAG and MARK sites (1986, 1990), Mid-Atlantic Ridge and a mechanism for Cu/Zn zonation in massive sulphide orebodies. *In* Hydrothermal Vents and Processes (L.M. Parson, C.L. Walker & D.R. Dixon, eds.). *Geol. Soc., Spec. Publ.* **87**, 77-86.

Eldridge, C.S., Barton, P.B., Jr. & Ohmoto, H. (1983): Mineral textures and their bearing on formation of the Kuroko orebodies. *Econ. Geol., Monogr.* **5**, 241-281.

Embley, R.W., Jonasson, I.R., Perfit, M.R., Franklin, J.M., Tivey, M.A., Malahoff, A., Smith, M.F. & Francis, T.J.G. (1988): Submersible investigation of an extinct hydrothermal system on the Galapagos Ridge: sulfide mounds, stockwork zone, and differentiated lavas. *Can. Mineral.* **26**, 517-539.

Falkner, K.K. & Edmond, J.M. (1990): Gold in seawater. *Earth Planet. Sci. Lett.* **98**, 208-221.

Fouquet, Y., Wafik, A., Cambon, P., Mével, C., Meyer, G. & Gente, P. (1993): Tectonic setting and mineralogical and geochemical zonation in the Snake Pit sulfide deposit (Mid-Atlantic Ridge at 23°N). *Econ. Geol.* **88**, 2018-2036.

Gammons, C.H. & Barnes, H.L. (1989): The solubility of Ag_2S in near-neutral aqueous sulfide solutions at 25 to 300°C. *Geochim. Cosmochim. Acta* **53**, 279-290.

Hannington, M.D. & Gorton, M.P. (1991): Analysis of sulfides for gold and associated trace metals by direct neutron activation with a low-flux reactor. *Geostandards Newsletter* **15**, 145-154.

———, HERZIG, P.M., SCOTT, S.D., THOMPSON, G. & RONA, P.A. (1991): Comparative mineralogy and geochemistry of gold-bearing sulfide deposits on the mid-ocean ridges. *Marine Geol.* **101**, 217-248.

———, ———, TIVEY, M.K., THOMPSON, G. & RONA, P.A. (1992): Hydrothermal reworking of sulfide deposits in the TAG Field, Mid-Atlantic Ridge: Evidence from the distribution of gold. *Eos (Trans. Am. Geophys. Union)* **73**, 530-531 (abstr.).

———, PETER, J.M. & SCOTT, S.D. (1986): Gold in seafloor polymetallic sulfide deposits. *Econ. Geol.* **81**, 1867-1883.

——— & SCOTT, S.D. (1988): Mineralogy and geochemistry of a hydrothermal silica–sulfide–sulfate spire in the caldera of Axial Seamount, Juan de Fuca Ridge. *Can. Mineral.* **26**, 603-625.

——— & ——— (1989a): Gold mineralization in volcanogenic massive sulfides: implications of data from active hydrothermal vents on the modern sea-floor. *Econ. Geol., Monogr.* **6**, 491-507.

——— & ——— (1989b): Sulfidation equilibria as guides to gold mineralization in volcanogenic massive sulfides: evidence from sulfide mineralogy and the composition of sphalerite. *Econ. Geol.* **84**, 1978-1995.

———, THOMPSON, G., RONA, P.A. & SCOTT, S.D. (1988): Gold and native copper in supergene sulphides from the mid-Atlantic Ridge. *Nature* **333**, 64-66.

HEKINIAN, R. & FOUQUET, Y. (1985): Volcanism and metallogenesis of axial and off-axis structures on the East Pacific Rise near 13°N: *Econ. Geol.* **80**, 221-249.

———, FRANCHETEAU, J. & BALLARD, R.D. (1985): Morphology and evolution of hydrothermal deposits at the axis of the East Pacific Rise. *Oceanologica Acta* **8**, 147-155.

HELGESON, H.C. (1969): Thermodynamics of hydrothermal systems at elevated temperatures and pressures. *Am. J. Sci.* **267**, 729-804.

HERZIG, P.M., HANNINGTON, M.D., FOUQUET, Y., VON STACKELBERG, U. & PETERSEN, S. (1993): Gold-rich polymetallic sulfides from the Lau back-arc and implications for the geochemistry of gold in seafloor hydrothermal systems of the S.W. Pacific. *Econ. Geol.* **88**, 2182-2209.

———, ———, SCOTT, S.D., MALIOTIS, G., RONA, P.A. & THOMPSON, G. (1991): Gold-rich sea-floor gossans in the Troodos ophiolite and on the Mid-Atlantic Ridge. *Econ. Geol.* **86**, 1747-1755.

HUSTON, D.L., BOTTRILL, R.S., CREELMAN, R.A., ZAW, KIM, RAMSDEN, T.R., RAND, S.W., GEMMELL, J.B., JABLONSKI, W., SIE, S. & LARGE, R.R. (1992): Geological and geochemical controls on the mineralogy and grain size of gold-bearing phases, eastern Australian volcanic-hosted massive sulfide deposits. *Econ. Geol.* **87**, 542-563.

——— & LARGE, R.R. (1989): A chemical model for the concentration of gold in volcanogenic massive sulfide deposits. *Ore Geol. Rev.* **4**, 171-200.

JEAN, G.E. & BANCROFT, G.M. (1985): An XPS and SEM study of gold deposition at low temperatures on sulphide mineral surfaces: concentration of gold by adsorption/reduction. *Geochim. Cosmochim. Acta* **49**, 979-987.

KRUPP, R.E. & SEWARD, T.M. (1987): The Rotokawa geothermal system, New Zealand: an active epithermal gold-depositing environment. *Econ. Geol.* **82**, 1109-1129.

LALOU, C., REYSS, J.L., BRICHET, E., ARNOLD, M., THOMPSON, G., FOUQUET, Y. & RONA, P.A. (1993): New age data for Mid-Atlantic ridge hydrothermal sites: TAG and Snakepit chronology revisited. *J. Geophys. Res.* **98**, 9705-9713.

———, THOMPSON, G., ARNOLD, M., BRICHET, E., DRUFFEL, E. & RONA, P.A. (1990): Geochronology of TAG and Snakepit hydrothermal fields, Mid-Atlantic Ridge: witness to a long and complex hydrothermal history. *Earth Planet. Sci. Lett.* **97**, 113-128.

LARGE, R.R., HUSTON, D.L., MCGOLDRICK, P.J., RUXTON, P.A. & MCARTHUR, G. (1989): Gold distribution and genesis in Australian volcanogenic massive sulfide deposits and significance for gold transport models. *Econ. Geol., Monogr.* **6**, 520-536.

LAROCQUE, A.C.L., HODGSON, C.J., CABRI, L.J. & JACKMAN, J.A. (1992): Application of SIMS analysis of pyrite to the study of metamorphic remobilization of Au in the Mobrun VMS deposit, Rouyn–Noranda, Quebec. *Geol. Assoc. Can. – Mineral. Assoc. Can., Program Abstr.* **17**, A63.

———, ———, ——— & ——— (1995): Ion-microprobe analysis of pyrite, chalcopyrite and pyrrhotite from the Mobrun VMS deposit in northwestern Quebec: evidence for metamorphic remobilization of gold. *Can. Mineral.* **33**, 373-388.

LEG 158 SHIPBOARD SCIENTIFIC PARTY (1995): Drilling an active hydrothermal system at the Mid-Atlantic Ridge. *Eos (Trans. Am. Geophys. Union)*, **76**, 361 (abstr.).

LYDON, J.W. (1984): Some observations on the morphology and ore textures of volcanogenic sulfide deposits of Cyprus. *Geol. Surv. Can., Pap.* **84-1A**, 601-610.

MANN, A.W. (1984): Mobility of gold and silver in lateritic weathering profiles: some observations from Western Australia. *Econ. Geol.* **79**, 38-49.

MORRISON, G.W., ROSE, W.J. & JAIRETH, S. (1991): Geological and geochemical controls on the silver content (fineness) of gold-silver deposits. *Ore Geol. Rev.* **6**, 333-364.

PARADIS, S., JONASSON, I.R., LE CHEMINANT, G.M. & WATKINSON, D.H. (1988): Two zinc-rich chimneys from the Plume Site, southern Juan de Fuca Ridge. *Can. Mineral.* **26**, 637-654.

RENDERS, P.J. & SEWARD, T.M. (1989a): The stability of hydrosulphido and sulphido-complexes of Au(I) and Ag(I) at 25°C. *Geochim. Cosmochim. Acta* **53**, 245-253.

_____ & _____ (1989b): The adsorption of thio gold (I) complexes by amorphous As_2S_3 and Sb_2S_3 at 25 and 90°C. *Geochim. Cosmochim. Acta* **53**, 255-267.

RONA, P.A., BOGDANOV, Y.A., GURVICH, E.G., RIMSKI-KORSAKOV, N.A., SAGALEVITCH, A.M., HANNINGTON, M.D. & THOMPSON, G. (1993b): Relict hydrothermal zones in the TAG hydrothermal field, Mid-Atlantic Ridge 26°N, 45°W. *J. Geophys. Res.* **98**, 9715-9730.

_____, HANNINGTON, M.D., RAMAN, C.V., THOMPSON, G., TIVEY, M.K., HUMPHRIS, S.E., LALOU, C. & PETERSEN, S. (1993a): Active and relict sea-floor hydrothermal mineralization at the TAG Hydrothermal Field, Mid-Atlantic Ridge. *Econ. Geol.* **88**, 1989-2017.

_____, _____ & THOMPSON, G. (1990): Evolution of hydrothermal mounds, TAG hydrothermal field, Mid-Atlantic Ridge 26°N, 45°W. *Eos (Trans. Am. Geophys. Union)* **71**, 1650 (abstr.).

SCOTT, S.D., CHASE, R.L., HANNINGTON, M.D., MICHAEL, P.J., MCCONACHY, T.F. & SHEA, G.T. (1990): Sulfide deposits, tectonics, and petrogenesis of Southern Explorer Ridge, northeast Pacific Ocean. *In Proc. Troodos '87, Ophiolite Symp.* (J. Malpas *et al.*, eds.). Geol. Surv. Dep., Nicosia, Cyprus (719-733).

SEWARD, T.M. (1976): The stability of chloride complexes of silver in hydrothermal solutions up to 350°C. *Geochim. Cosmochim. Acta* **40**, 1329-1341.

_____ (1984): The transport and deposition of gold in hydrothermal systems. *In* The Geology, Geochemistry, and Genesis of Gold Deposits; Proc. Gold'82 (Harare, Zimbabwe) (R.P. Foster, ed.). Balkema, Rotterdam, The Netherlands (165-181).

SHENBERGER, D.M. & BARNES, H.L. (1989): Solubility of gold in aqueous sulfide solutions from 150 to 350°C. *Geochim. Cosmochim. Acta* **53**, 269-278.

SHIMAZAKI, Y. (1974): Ore minerals of the Kuroko-type deposits. *Soc. Mining Geologists Japan, Spec. Issue* **6**, 311-322.

SUGAKI, A., SCOTT, S.D., HAYASHI, K. & KITAKAZE, A. (1987): Ag_2S solubility in sulfide solutions up to 250°C. *Geochem. J.* **21**, 291-305.

THOMPSON, G., HUMPHRIS, S.E., SCHROEDER, B., SULANOWSKA, M. & RONA, P.A. (1988): Active vents and massive sulfides at 26°N (TAG) and 23°N (Snakepit) on the Mid-Atlantic Ridge. *Can. Mineral.* **26**, 697-711.

TIVEY, M.K., HUMPHRIS, S.E., THOMPSON, G., HANNINGTON, M.D. & RONA, P.A. (1995): Deducing patterns of fluid flow and mixing within the active TAG mound using mineralogical and geochemical data. *J. Geophys. Res.*, **100**, 2527-2556.

_____, _____, _____, WARD, K.A., HANNINGTON, M.D. & RONA, P.A. (1990): Mineral precipitation at the TAG (26°N) and Snakepit (23°N) hydrothermal sites, Mid-Atlantic Ridge. *Eos (Trans. Am. Geophys. Union)* **71**, 1650 (abstr.).

_____, THOMPSON, G., HUMPHRIS, S.E., HANNINGTON, M.D. & RONA, P.A. (1992): Similarities between the TAG active hydrothermal mound, MAR 26°N and ore deposits of the Troodos ophiolite. *Eos (Trans. Am. Geophys. Union)* **73**, 360 (abstr.).

VON DAMM, K.L., EDMOND, J.M., GRANT, B., MEASURES, C.I., WALDEN, B. & WEISS, R.F. (1985): Chemistry of submarine hydrothermal solutions at 21°N, East Pacific Rise. *Geochim. Cosmochim. Acta* **49**, 2197-2220.

WEBSTER, J.G. (1986): The solubility of gold and silver in the systems Au–Ag–S–O_2–H_2O at 25°C and 1 atm. *Geochim. Cosmochim. Acta* **50**, 1837-1845.

ZIERENBERG, R.A., KOSKI, R.A, MORTON, J.L., BOUSE, R.M. & SHANKS, W.C., III (1993): Genesis of massive sulfide deposits on a sediment-covered spreading center, Escanaba Trough, Southern Gorda Ridge. *Econ. Geol.* **88**, 2069-2098.

_____ & SCHIFFMAN, P. (1990): Microbial control of silver mineralization at a sea-floor hydrothermal site on the Northern Gorda Ridge. *Nature* **348**, 155-157.

Received March 22, 1995, revised manuscript accepted June 28, 1995.